Chemosphere 254 (2020) 126792

Contents lists available at ScienceDirect

Chemosphere

journal homepage: www.elsevier.com/locate/chemosphere

Comparative developmental toxicity of iron oxide nanoparticles and ferric chloride to zebrafish (*Danio rerio*) after static and semi-static exposure

Aryelle Canedo Pereira [a], Bruno Bastos Gonçalves [a], Rafaella da Silva Brito [a], Lucélia Gonçalves Vieira [b], Emília Celma de Oliveira Lima [c], Thiago Lopes Rocha [a, *]

[a] Laboratory of Environmental Biotechnology and Ecotoxicology, Institute of Tropical Pathology and Public Health, Federal University of Goiás, Goiania, Goiás, Brazil
[b] Department of Morphology, Institute of Biological Sciences, Federal University of Goiás, Goiania, Goiás, Brazil
[c] Chemistry Institute, Federal University of Goiás, Goiania, Goiás, Brazil

HIGHLIGHTS

- Differential developmental toxicity of γ-Fe_2O_3 NPs and iron ions in zebrafish.
- Embryotoxicity of γ-Fe_2O_3 NPs depends on the exposure condition (static and semi-static).
- Semi-static exposure induced high embryotoxicity than static exposure.
- γ-Fe_2O_3 NPs induced several cardiotoxic effects on zebrafish embryos.

GRAPHICAL ABSTRACT

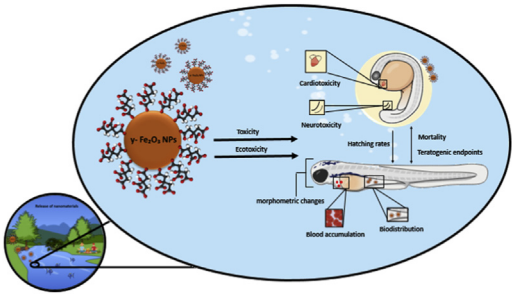

ARTICLE INFO

Article history:
Received 15 January 2020
Received in revised form
2 April 2020
Accepted 12 April 2020
Available online 25 April 2020

Handling Editor: Tamara S. Galloway

Keywords:
Nanoecotoxicology
Nanomaterials
Cardiotoxicity
Biomarkers
Embryotoxicity
Zebrafish embryotoxicity test (ZET)

ABSTRACT

Iron oxide nanoparticles (IONPs) are used in several medical and environmental applications, but their mechanism of action and hazardous effects to early developmental stages of fish remain unknown. Thus, the present study aimed to assess the developmental toxicity of citrate-functionalized IONPs (γ-Fe_2O_3 NPs), in comparison with its dissolved counterpart, in zebrafish (*Danio rerio*) after static and semi-static exposure. Embryos were exposed to environmental concentrations of both iron forms (0.3, 0.6, 1.25, 2.5, 5 and 10 mg L^{-1}) during 144 h, jointly with negative control group. The interaction and distribution of both Fe forms on the external chorion and larvae surface were measured, following by multiple biomarker assessment (mortality, hatching rate, neurotoxicity, cardiotoxicity, morphological alterations and 12 morphometrics parameters). Results showed that IONPs were mainly accumulated on the zebrafish chorion, and in the digestive system and liver of the larvae. Although the IONPs induced low embryotoxicity compared to iron ions in both exposure conditions, these nanomaterials induced sub-lethal effects, mainly cardiotoxic effects (reduced heartbeat, blood accumulation in the heart and pericardial edema). The semi-static exposure to both iron forms induced high embryotoxicity compared to static exposure, indicating that the nanotoxicity to early developmental stages of fish depends on the

* Corresponding author. Universidade Federal de Goiás, Instituto de Patologia Tropical e Saúde Pública, Rua 235, Setor Universitário, CEP: 74605050, Goiania, Goiás, Brazil.
E-mail address: thiagorochabio20@ufg.br (T.L. Rocha).

https://doi.org/10.1016/j.chemosphere.2020.126792

exposure system. This is the first study concerning the role of the exposure condition on the developmental toxicity of IONPs on fish species.

1. Introduction

Nanomaterials (NMs) have been produced and incorporated in commercial products on a large scale, which consequently increases their release into the aquatic environment (Giese et al., 2018). It is estimated that more than 10,000 tons/year of NMs are released into the environment (Salieri et al., 2018). In 2050, the concentration of NMs in fresh and marine waters, sediments and soils is likely to be 1000 times higher (Giese et al., 2018). These emerging pollutants have nano-specific properties that can induced hazardous effects to the environment and human health (Joo and Zhao, 2017). Among these NMs, iron oxide nanoparticles (IONPs) have been used in several medical and environmental applications, such as cancer treatment by hyperthermia (Giustini et al., 2010), contrast agents (Fatima and Kim, 2018), drug delivery (Laurent et al., 2014), nanoremediation (Hjorth et al., 2017) and water treatment (Xu et al., 2012). The main types of IONPs with biological and environmental applications are magnetite (Fe_3O_4 NPs), hematite (α-Fe_2O_3 NPs) and maghemite (γ-Fe_2O_3 NPs) (Su, 2017), especially due to their physicochemical properties, such as high surface area, small size, optimum crystallization, magnetism, adsorption capacity and biocompatibility (Xu et al., 2012; Vikram et al., 2017; Babić-Stojić et al., 2017).

Despite the numerous advantages of IONPs, previous studies have indicated its environmental transformation and hazardous impact to aquatic organisms and human health (Joo and Zhao, 2017; Qualhato et al., 2017, 2018). After their release into the aquatic environment, IONPs can undergo physical, chemical and biological transformations, including homoaggregation, heteroaggregation with natural organic matter (NOM), oxidative dissolution, aging through oxidation-reduction reactions, bio-reduction and adsorption with other pollutants (Trojan horse effect) (Moore, 2006; Patil et al., 2016; Lei et al., 2018). Regarding its potential ecotoxicological impact, the environmental concentration (0.3 mg L^{-1}) of citrate-functionalized γ-Fe_2O_3 NPs (3.97 nm) induced genotoxic (DNA damage) and mutagenic effects (micronucleus and erythrocytic nuclear alterations), and hepatic alterations (i.e., micro and macrovesicular steatosis, melanomacrophage aggregates, exudate and hemorrhagic foci) in guppy (*Poecilia reticulata*) during 21 days of exposure (Qualhato et al., 2017, 2018). In addition, the exposure of zebrafish embryos to uncoated γ-Fe_2O_3 NPs (30 nm; 0.1–100 mg L^{-1}) for 168 h induced pericardial edema, tissue ulceration and spinal curvature (Zhu et al., 2012). The IONP toxicity to fish also depends on the synthesis method. IONPs obtained by coprecipitation (15.58 nm; 79.04 and 278.67 ppm) induced bioaccumulation and increased erythrocyte damage in adult zebrafish during 96 h of exposure, while those obtained by the green synthesis method (21.34 nm; 79.04 and 278.67 ppm) inhibited the Na^+/K^+-ATPase activity in a concentration dependent pattern (Suganya et al., 2018). On the other hand, the role of the exposure condition on the embryotoxicity of IONPs on fish species remain unknow.

The zebrafish embryotoxicity test (ZET) has been indicated as a suitable approach to assess the NM toxicity on human and environmental health (Pereira et al., 2019), as well as a preclinical *in vivo* screening model for nanomedicines (Sieber et al., 2019). According to the guideline nº 236 of the Organization for Economic Cooperation and Development (OECD) (OECD, 2013), the semi-static exposure system is recommended for volatile substance and materials with high precipitation rate. On the other hand, few studies perform medium exchange during ZET for nanotoxicity assessment (Pereira et al., 2019). Thus, the lack of standardization of tests may cause interference with the toxicity results of NMs (Lammer et al., 2009; Beekhuizen et al., 2015; Truong et al., 2011).

Zebrafish (*D. rerio*) has been an excellent animal model for the analysis of multiple biomarkers of NM toxicity (Fako and Furgeson, 2009; Harper et al., 2011; Lin et al., 2013; Bugel et al., 2014; Chakraborty et al., 2016; Haque and Ward, 2018; Pereira et al., 2019), especially due to its numerous advantages, such as easy maintenance in the laboratory conditions, small size, high egg production, embryos are transparent which allows to follow their whole development, and fast development when compared to other vertebrate models (Lammer et al., 2009; Giannaccini et al., 2014; Beekhuizen et al., 2015; Sobanska et al., 2018). Information networks such as ZFIN (zfin.org), combined with the fact that embryos can be cryopreserved, ensure quick and easy access to transgenic zebrafish lines (Sieber et al., 2019). In addition, its genetic material is 70% similar to humans (Howe et al., 2013), ensuring a similarity between developmental processes, cell signalling, cell structures, anatomy and physiology (Rubinstein, 2003; Hill et al., 2005; Kelkar et al., 2014).

In this context, the present study aimed to assess the developmental toxicity of citrate-functionalized γ-Fe_2O_3 NPs and its dissolved counterpart on zebrafish, using two aquatic exposure systems (static and semi-static exposure). Thus, the hypothesis that the embryotoxicity of citrate-functionalized γ-Fe_2O_3 NPs in zebrafish is dependent on exposure condition was tested. In addition, the present study analyzed the differential developmental toxicity of γ-Fe_2O_3 NPs and their dissolved counterpart. To the best of our knowledge, the present study is the first report on the role of the exposure condition (static and semi-static aquatic systems) on toxicity of IONPs during the early developmental stage of fish. Assumingly, studies such as the present one broadens the possibility of using the ZET on analysis and classification of the toxicity and environmental impact of NMs.

2. Material and methods

2.1. Synthesis and characterization of IONPs

Citrate-functionalized maghemite (γ-Fe_2O_3 NPs) were synthesized according to Unal et al. (2010) and Zia et al. (2016) with some modifications, such as described by Qualhato et al. (2017). After synthesis, NPs were characterized in terms of morphology and individual diameter (D_{TEM}) by Transmission Electron Microscopy (TEM), while the hydrodynamic diameter (D_h) and surface charge (zeta potential) were analyzed by dynamic light scattering (DLS) and electrophoretic light scattering (ELS), respectively. The IONPs were also characterized by X-ray diffraction (XDR), KBr tablet infrared spectroscopy (IR-KBR) and ultraviolet–visible (UV–vis)

spectroscopy, as previously described by Qualhato et al. (2017, 2018).

2.2. Zebrafish

Adult wild-type zebrafish with 6–24 months (total length = 3 ± 5 cm) were obtained and maintained in the zebrafish facilities of the Institute of Tropical Pathology and Public Health (IPTSP) from Federal University of Goiás (UFG), using in polycarbonate aquariums (11.5 cm × 34.5 cm x 15.5 cm) (Alesco®) with constant water circulation (3 L), under controlled conditions of water temperature (26 ± 1 °C), pH (7.0 ± 0.5), dissolved oxygen (>80%), and photoperiod (light: dark cycle 14:10 h), such as recommended by Dammski et al. (2011). Animals were fed daily with commercial food (Cardume® 36%; VB alimentos) and *Artemia* sp. nauplii. Brine shrimp (*Artemia* sp.) eggs were hatched in the laboratory condition according to Avdesh et al. (2012). The maintenance of adult animals and the execution of ZET followed the regulations of OECD Guide 236 (OECD, 2013), and were approved by the Institutional Committee of Animal Use and Care from UFG (nº 094/17).

2.3. Zebrafish embryotoxicity test (ZET)

The ZET was performed according to OECD Guideline nº 236 (OECD, 2013), Lammer et al. (2009) and Pereira et al. (2019). After reproduction induction in breeding tanks (Alesco®) using males (n = 12) and females (n = 4) at rate of 3:1, embryos were transferred to a Petri dish, washed with reconstituted water (ISO, 1996) and the viable embryos (up to 4 h post-fertilization – hpf; 4 to 128-cell stage) were selected using photomicroscope (Leica DM 750) according to Kimmel et al. (1995) and Lammer et al. (2009).

For the bioassays, zebrafish embryos were distributed in 24-well microplates (Kasvi®), using 1 embryo *per* well containing 2 mL of each nominal concentration of citrate functionalized γ-Fe_2O_3 NPs or ferric chloride (0.31 = 0.3; 0.62 = 0.6, 1.25, 2.5, 5.0 and 10 mg L^{-1}), jointly with the negative control group (reconstituted water) (Fig. 1). The positive control group was exposed to 3,4-dichloroaniline (3.7 mg L^{-1}) under static conditions, according to Lammer et al. (2009) The iron concentrations used are environmentally relevant and are below the maximum allowable concentration in the aquatic environment (15 mg L^{-1}) according to CONAMA Resolution n. 430/2011 (Brasil, 2011). Furthermore, similar concentrations were used in previous studies about the ecotoxicity of IONPs on fish species (Ates et al., 2016; Qualhato et al., 2017). The exposure was conducted in triplicate (3 microplates with 10 embryos *per* group; totalizing 30 embryos *per* experimental condition) using static (without exposure solution renewal) and semi-static conditions (exposure solution renewed every 24 h with redosing of concentrations of both iron forms) during 144 h under controlled pH (7.2 ± 0.2), photoperiod (14:10 h light/dark cycles) and temperature (27 ± 1 °C) in BioOxygen Demand (BOD) incubator (SOLAB SL-224/120, Brazil). For the test validation, the fertilization rate >90% and the negative control group survival >90% were considered (ISO, 1996; 2007; OECD, 2013; Lammer et al., 2009).

2.4. Interaction of IONPs to embryo chorion and larvae surface

Zebrafish embryos (n = 4) were selected after 48 h exposure (before hatching) to evaluate the interaction of IONPs with the chorion. The larvae (n = 4) were selected at the end of the exposure period (144 h) to evaluate the interaction of the IONPs with the surface of the larvae from control group and after exposure to IONPs at 1.25 and 10 mg L^{-1} and iron ions at 1.25 mg L^{-1}, since that the iron ions at 2.5 mg L^{-1} (semi-static exposure) induced 100% mortality. Embryos and larvae were immediately fixed by immersion in 10% paraformaldehyde for 4 h, washed in 0.2 M PBS buffer at pH 7.2, dehydrated through increasing ethanol gradient (70 and 100%) and dried with liquid carbon dioxide (CO_2) in critical-point drier (Autosamdri® 815 A). Dried materials were sputtered-coated with gold in a Denton Vacuum Sputter Coater (Denton Vacuum, LLC, Moorestown, NJ, USA), and analyzed using a scanning electron microscope (SEM) (Jeol JSM-6610) coupled with energy dispersive X-ray spectroscopy (EDS) (Thermo scientific NSS Spectral Imaging).

2.5. Accumulation

After the exposure period (144 h) to citrate-functionalized γ-Fe_2O_3 NPs or ferric chloride, zebrafish larvae (n = 10 *per* experimental group) were fixed by immersion in 4% buffered paraformaldehyde at pH 7.2 for 4 h, washed with 0.2 M PBS buffer at pH 7.2 and stored in 70% ethanol at 4 °C. Photographs of the lateral region of zebrafish larvae (0.31, 0.62, 1.25, 2.5, 5.0 and 10 mg L^{-1}) at 500 × magnification were taken in the photomicroscope (Leica DM 750) coupled to the image capture system (Leica Microsystem LAS EZ). The image analysis was based on the procedure described by Wu et al. (2008) with modifications. The accumulation area was determined using Image J software according to following equation: accumulation area = iron accumulation area in the intestinal system/total area of the intestinal system of larvae.

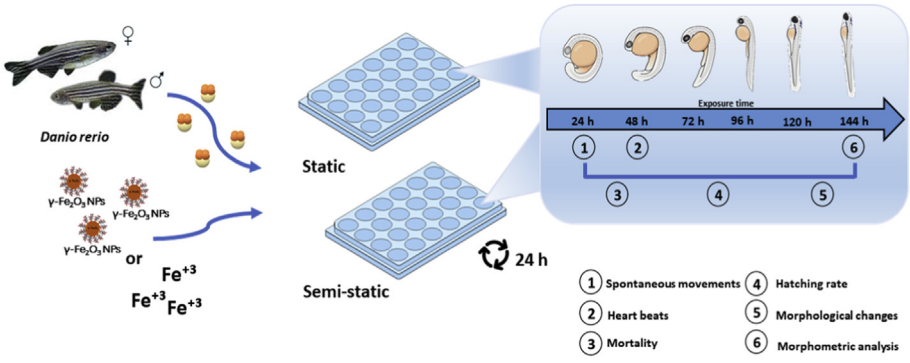

Fig. 1. Experimental design and analysis of multiple biomarkers during the zebrafish embryotoxicity test (ZET). The developmental toxicity of citrate-functionalized γ-Fe_2O_3 NPs and iron ions was analyzed during 144 h under static (without exposure medium renewal) and semi-static conditions (exposure medium renewed every 24 h with redosing of concentrations of both iron forms).

2.6. Biomarker responses

The experimental design and multiple biomarker assessment during the ZET are in Fig. 1. During the exposure period, embryos were analyzed daily (24, 48, 72, 96, 120 and 144 h) using a photomicroscope (Leica DM 750) associated with the LEICA ICC50 HD camera and LAS EZ software. A battery of biomarkers was analyzed, such as mortality and hatching rate (24–144 h), spontaneous contraction frequency (SCF) (24 h), heart beat rate (48 h), morphological alterations frequency (24–144 h) and biometric parameters (144 h).

The zebrafish embryos and larvae with no spontaneous movements, heartbeat or coagulated were as considered dead (Lammer et al., 2009). The mortality rate (%) was determined using the following equation: mortality rate (%) = (number of dead embryos/total number of embryos) *x* 100. The hatching rate (%) was calculated through the following equation: hatching rate (%) = (number of hatched embryos/total number of embryos) *x* 100. The morphological alterations were measured by determining the frequency of embryos or larvae with blood accumulation in the heart, deformation of the yolk sac, edema of the pericardium, spinal curvature, swimming bladder deformity and tail malformation, according to Lammer et al. (2009) and Beekhuizen et al. (2015). The total morphological alteration frequency is the sum of all morphological changes. In addition, these morphological alterations were classified into four reaction pattern (Rp): circulatory changes (Rp1), pigmentation and integumentary changes (Rp2), musculoskeletal disorders (Rp3) and yolk sac alterations (Rp4), as described by Pereira et al. (2019).

2.6.1. Neurotoxicity and cardiotoxicity

The neurotoxicity was determined through the spontaneous contraction frequency (SCF) (n^o min^{-1}) in embryos (26–28 hpf) after 24 h of exposure according to Babić et al. (2017). The SCF have been indicated as suitable sublethal endpoint to the potential neurotoxicity of substances (Weichert et al., 2017; Krzykwa et al., 2019). The cardiotoxicity was determined through the heart beat rate *per* minute (bpm) in embryos (50–52 hpf) after 48 h of exposure (Babić et al., 2017), especially due to the reduced movement and transparency of the embryos. Briefly, for analysis of both parameters, embryo was placed on a microscope slide in a thin layer of reconstituted water (ISO, 1996) and immediately positioned horizontally using a disposable transfer pipette. Each embryo was analyzed during 60 s (n = 30 embryos *per* experimental group) using a photomicroscope (Leica DM 750) coupled to an image capture system (Leica Microsystem LAS EZ).

2.6.2. Morphometric analysis

At the end of the exposure period (144 h), the larvae were fixed by immersion in 4% paraformaldehyde pH 7.2 for 4 h, washed in 0.2 M PBS buffer pH 7.2 and stored in 70% alcohol at 4 °C. Afterwards photographs of the lateral and dorsal region of zebrafish larvae (n = 10 *per* experimental group) were obtained using the photomicroscope (Leica DM 750) coupled to the image capture system (Leica Microsystem LAS EZ). Four categories of morphometric parameters (n = 12) were measured in the larvae using the Image J software, accordingly Malafaia et al. (2020): (*i*) sensory (eye area – AO, minimum interocular distance – DI and maximum interocular distance – DIM); (*ii*) physiological (heart area – AC, swimming bladder area – AB, and vitelline sac area – AV); (*iii*) structural/skeletal (head height – CA, head width – CL, head depth – CP, distance from mouth to anus – DAB); (*iv*) structural/muscular (angle between myosepts and distance between myosepts) (see Supplementary material - Fig. S1).

2.7. Statistical analysis

The graphs were organized using the Prism 7 GraphPad® software, while the statistical analyzes were performed using the R software. Normality and homoscedasticity were verified with the Shapiro-Wilk and Levene tests, respectively. Heart beat rate, spontaneous movement rate and morphometric parameters were analyzed by one-way ANOVA, following by Tukey post hoc tests. Mortality rate, hatching rate and teratogenic effects were analyzed using multiple factor ANOVA (Underwood, 1997). Log rank analysis was performed to assess differences in trends of survival analysis. Results were considered when $p < 0.05$.

3. Results and discussion

3.1. IONP characterization

IONPs used in the present study were previously characterized by Qualhato et al. (2017, 2018). TEM results showed the citrate-functionalized γ-Fe_2O_3 NPs with rounded shape, excellent crystallinity and a D_{TEM} of 3.97 ± 0.85 nm. The FTIR spectrum demonstrated two bands at 1594 cm^{-1} and 1380 cm^{-1}, confirming the functionalization of γ-Fe_2O_3 NPs by citrate. The citrate confers negative surface charge to IONPs in reconstituted water (−19.5 ± 6.5 mV) and Milli-Q water (−51.1 ± 7 mV). Higher hydrodynamic diameter was observed in reconstituted water (21.4 ± 0.39 nm) compared to Milli-Q water (14.11 ± 0.2 nm). Atomic absorption spectrophotometric analysis showed that the total iron content in the γ-Fe_2O_3 NPs stock dispersion was 6.8 mg mL^{-1}. The XRD analysis showed two broad picks (311 and 440) with low intensity, indicating cubic spinel phase and small particles (Teja and Koh, 2009; Wu et al., 2015). In addition, the XRD pattern along with the UV–Vis-Near IR allowed to characterize maghemite-type NPs. The UV–Vis-Near IR of the γ-Fe_2O_3 NPs suspension showed the characteristic absorption near the wavelength region attributed to the presence of Fe (III) ions in a tetrahedral site, confirming the transformation of magnetite to maghemite NPs by oxidation. Overall results showed that the zebrafish embryos and larvae were exposed to aggregates of maghemite with negative surface charge. Similarly, the aggregation of γ-Fe_2O_3NPs in aquatic systems was reported in previous studies (Zhu et al., 2012; Qualhato et al., 2017, 2018; Lei et al., 2018).

3.2. Nanobiointeraction on embryo and larvae surface

SEM followed by EDS analysis showed the presence of γ-Fe_2O_3 NPs and iron adhered to the embryo chorion after 48 h of exposure (Fig. 2). Results indicated that the IONP interaction with the zebrafish embryo chorion may be mediated by three potential processes: (*i*) binding to the chorion surface; (*ii*) binding and blocking of chorion pore canals; (*iii*) passing through the chorion pore canals (Fig. 2). Glycoproteins and carbohydrates present on the chorion surface may interact with IONPs, promoting their adhesion to the embryo surface, as well as reducing their capture and toxicity, such as observed with SiO_2 NPs (Chao et al., 2018), polystyrene NPs (Pomeren et al., 2017; Lee et al., 2019), and fluorescent silica NPs (Fent et al., 2010). However, further studies are needed on the mechanism of interaction of these molecules with NMs.

Although the zebrafish chorion has been indicated as a selective barrier to the entry of NMs into zebrafish embryos (Cheng et al., 2007; Pomeren et al., 2017), the citrate-functionalized IONP aggregates have small diameter in reconstituted water (21.4 ± 0.39 nm) when compared to chorion pore size (500–700 nm) (Rawson et al., 2001), confirming that the γ-Fe_2O_3 NPs, being small in size compared to other NMs, are easier to cross

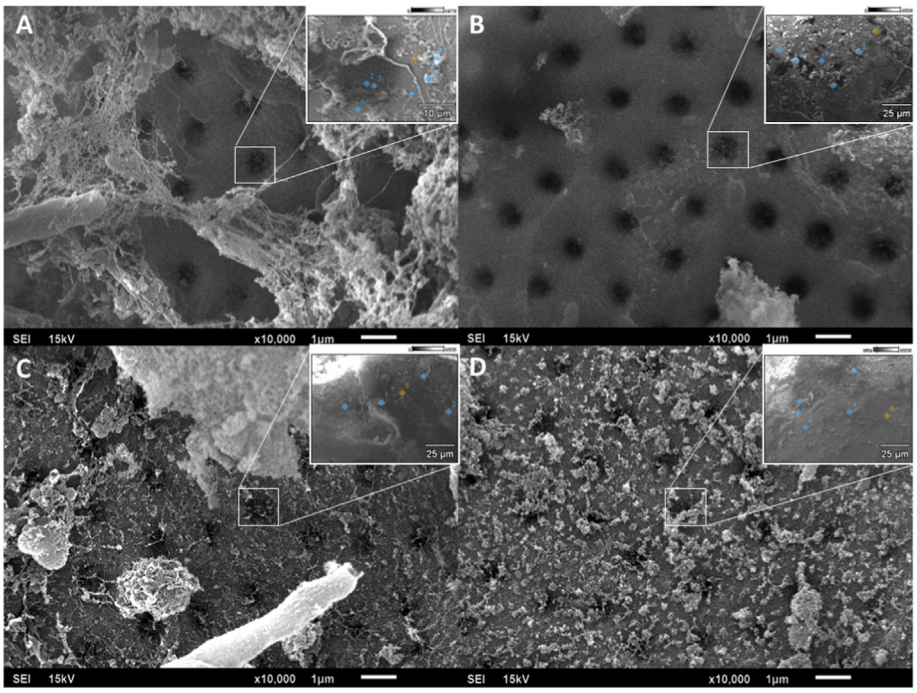

Fig. 2. Scanning Electron Microscopy (SEM) of zebrafish embryo chorion from control group and after exposure to γ-Fe_2O_3 nanoparticle (IONPs) and iron ions for 48 h. (A) Control. (B) Iron ions at 1.25 mg L^{-1}. (C) IONP at 1.25 mg L^{-1}. (D) IONP at 10 mg L^{-1}. Scale bar = 1 μm.

the chorion barrier (Cheng et al., 2007). Furthermore, the adherence and blocking of chorion pore canals by particles can reduce the gas exchange of the embryos, leading to pre-hatching hypoxia changes (Silva et al., 2018; Malafaia et al., 2019). In addition, high IONP aggregates adhered to the zebrafish chorion was observed after exposure to γ-Fe_2O_3 NPs at high concentration (10 mg L^{-1}) (67%) compared to low concentration (1.25 mg L^{-1}) (20%), indicating that the adherence was concentration-dependent (Fig. 3).

After hatching (48–72 hpf), the zebrafish larvae can interact and capture IONPs through the digestive system and gills. In addition, adherence of IONPs with skin and eyes of the larvae was also confirmed by SEM followed by EDS (Fig. 4). Larvae exposed to γ-Fe_2O_3 NPs and ferric chloride for 144 h showed iron aggregates in the eye, heart, intestinal tract and tail regions. The zebrafish larvae exposed to γ-Fe_2O_3 NPs at 1.25 mg L^{-1} showed NP aggregates adhered to eye (40%), tail (40%), heart (20%) and abdomen (10%), while those exposed to γ-Fe_2O_3 NPs at 10 mg L^{-1} showed NP aggregates mainly deposited in the heart (20%), eyes (10%), abdomen (10%) and tail (10%) (Fig. 4). Similarly, the larvae exposed to iron ions at 1.25 mg L^{-1} showed iron mainly deposited in the eye (50%), abdomen (40%), heart (30%) and tail (20%) (Fig. 4), confirming the interaction and adhesion of both iron forms on the larvae surface.

3.3. Accumulation

Both iron forms were accumulated mainly in the intestinal tract of zebrafish larvae in a concentration dependent pattern (Fig. 5). Larvae exposed to γ-Fe_2O_3 NPs at 10 mg L^{-1} showed higher accumulation area when compared to control group and other IONP and iron ion concentrations (Fig. 5G). Similarly, previous studies have reported accumulation of several NPs in the zebrafish intestinal tract, such as Ag NPs (Cambier et al., 2018), quantum dots (Chen et al., 2017a, 2017b), PS NPs (Pitt et al., 2018) and fullerenes (Della Torre et al., 2018). The IONP accumulation in the intestinal tract was also reported for invertebrate species, such as *Ceriodaphnia dubia* (Hu et al., 2012) and *Daphnia magna* (Magro et al., 2018). The intestinal tract has digestive, absorptive, secretory and protective functions (Bergin and Witzmann, 2013; Cheng et al., 2016). After ingestion, NPs can interact with the mucosa of the intestinal tract, as well as be absorbed, reach the bloodstream, and distribute to other organs. NPs can induce changes in physiological, metabolic and immunological functions (Bergin and Witzmann, 2013; Ates et al., 2013). As for example, TiO_2 NPs induced physiological changes in zebrafish larvae (Yang et al., 2017), CuO NPs promoted alterations in the zebrafish immune system (Aksakal and Ciltas, 2019) and polystyrene NPs caused metabolic changes in larvae of zebrafish (Brun et al., 2019).

Although the accumulation, metabolism and elimination kinetics of IONPs have not been described in fish, after distribution to other organs in BALB/c mice such as the liver and spleen, IONPs are captured by the mononuclear phagocytic system via endocytosis by Kupffer cells and spleen macrophages (Bostan et al., 2016; Feng et al., 2018). After phagocytosis, IONPs can be degraded by Kupffer cell lysosomes and spleen macrophages, releasing iron ions that interfere with iron homeostasis (Patil et al., 2015). Iron ions released by IONP degradation can participate in the Fenton Reactions and produce hydroxyl radicals, which are extremely toxic to cells, causing oxidative stress, inducing damage to cell organelles, altering their cell functions, and causing cell death (Wang et al., 2013; Lei et al., 2018). However, iron overload exceeds the body's ability to store iron ions, and these free iron ions lead to the reactive oxygen species (ROS) production (Voinov et al., 2011; Yang et al., 2015). The oxidative stress induced by IONP exposure was reported to several fish species, such as *Oryzias latipes* (Li et al., 2009), *Oreochromis niloticus* (Ates et al., 2016) and *P. reticulata* (Qualhato et al., 2017). In addition, in mammal models, IONP overload (Bostan et al., 2016; Feng et al., 2018) and iron (Parkes et al., 1993; Lekawanvijit and Chattipakorn, 2009) primarily affects the heart, which is one of the major organs that IONPs and iron have affinity, inducing myocardial injury, which can cause decreased heart rate, bleeding, and other effects on the heart (Parkes et al., 1993; Lekawanvijit and Chattipakorn, 2009; Bostan et al., 2016), such as

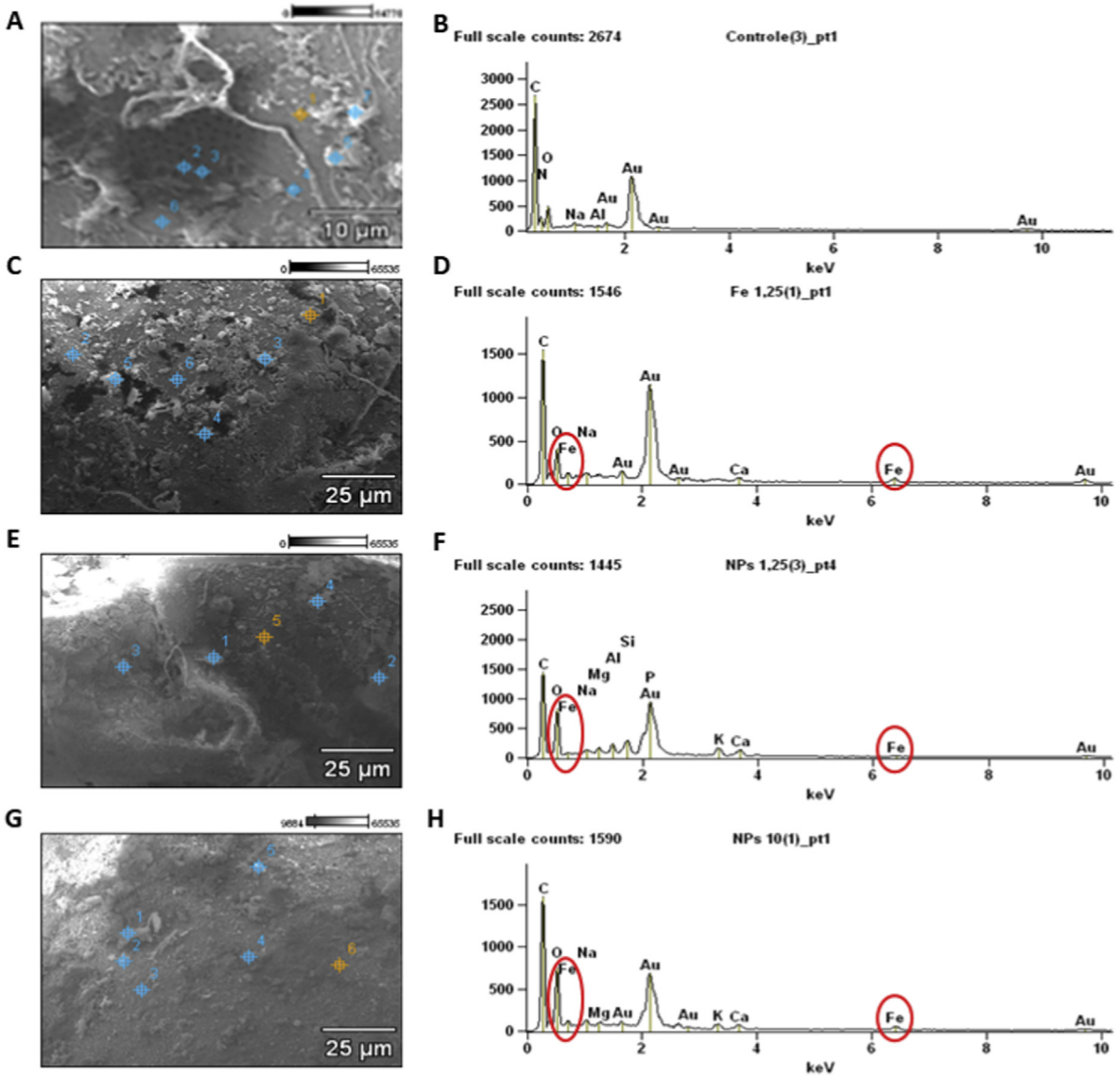

Fig. 3. Energy Dispersive X-Ray Spectroscopy (EDS) and Scanning Electron Microscopy (SEM) of zebrafish embryos chorion from control group and after exposure to γ-Fe_2O_3 nanoparticle (IONPs) and iron ions for 48 h. (A–B) Control. (C–D) Iron ions at 1.25 mg L^{-1}. (E–F) IONP at 1.25 mg L^{-1}. (G–H) IONP at 10 mg L^{-1}. The numbers indicate the region analyzed in relation to the accumulation. Scale bar = 25 µm.

observed in the present study.

3.4. Zebrafish embryotoxicity test - ZET

3.4.1. Mortality and hatching rate

The exposure of zebrafish embryos to γ-Fe_2O_3 NPs induced low mortality when compared to iron ions under static and semi-static exposure. After 144 h of static exposure, the mortality rate of embryos exposed to γ-Fe_2O_3 NPs at 0.3 mg L^{-1} was similar to the control group ($p > 0.05$; Fig. 6). However, γ-Fe_2O_3 NPs under static (0.6–10 mg L^{-1}) and semi-static exposure (0.3–10 mg L^{-1}) induced high mortality rate when compared to control group ($p < 0.05$; Fig. 6). Similarly, the static and semi-static exposure to iron ions (0.3–10 mg L^{-1}) induced high mortality rate in zebrafish embryos than unexposed ones ($p < 0.05$; Fig. 6). The embryo mortality in the positive control was 100%, as previously recommended by Lammer et al. (2009). In addition, the embryotoxicity of IONPs and iron ions was time and concentration dependent, such as indicated by Zhu et al. (2012). Both iron forms at 2.5, 5.0 and 10 mg L^{-1} induced high mortality when compared to the 0.3, 0.6, 1.25 mg L^{-1} ($p < 0.05$; Fig. 6). Based on observed results, the type of exposure influences the nanotoxicity during the early developmental of fish species. OECD guideline nº 236 (OECD, 2013) does not specify medium renewal in NM exposures, indicating only that in cases of volatile or highly adsorbed substances, medium renewal should be performed. The results showed the importance of a specific guideline to perform tests with NMs, since the exposure conditions influence the embryotoxicity of NMs (Pereira et al., 2019).

The static and semi-static exposure to both iron forms did not influence the hatching rate of zebrafish embryos ($p > 0.05$; Fig. 7), indicating that γ-Fe_2O_3 NPs and iron ions did not alter the hatching mechanism of embryos. Similarly, no effect on hatching rate was observed on zebrafish exposed to Pt NPs (Asharani et al., 2011), CeO_2 NPs (Wehmas et al., 2015), SnO_2 NPs (Wehmas et al., 2015) and CdSe (Chen et al., 2017a, 2017b). In opposite, others metal-based NPs inhibited the zebrafish hatching, such as Ag NPs

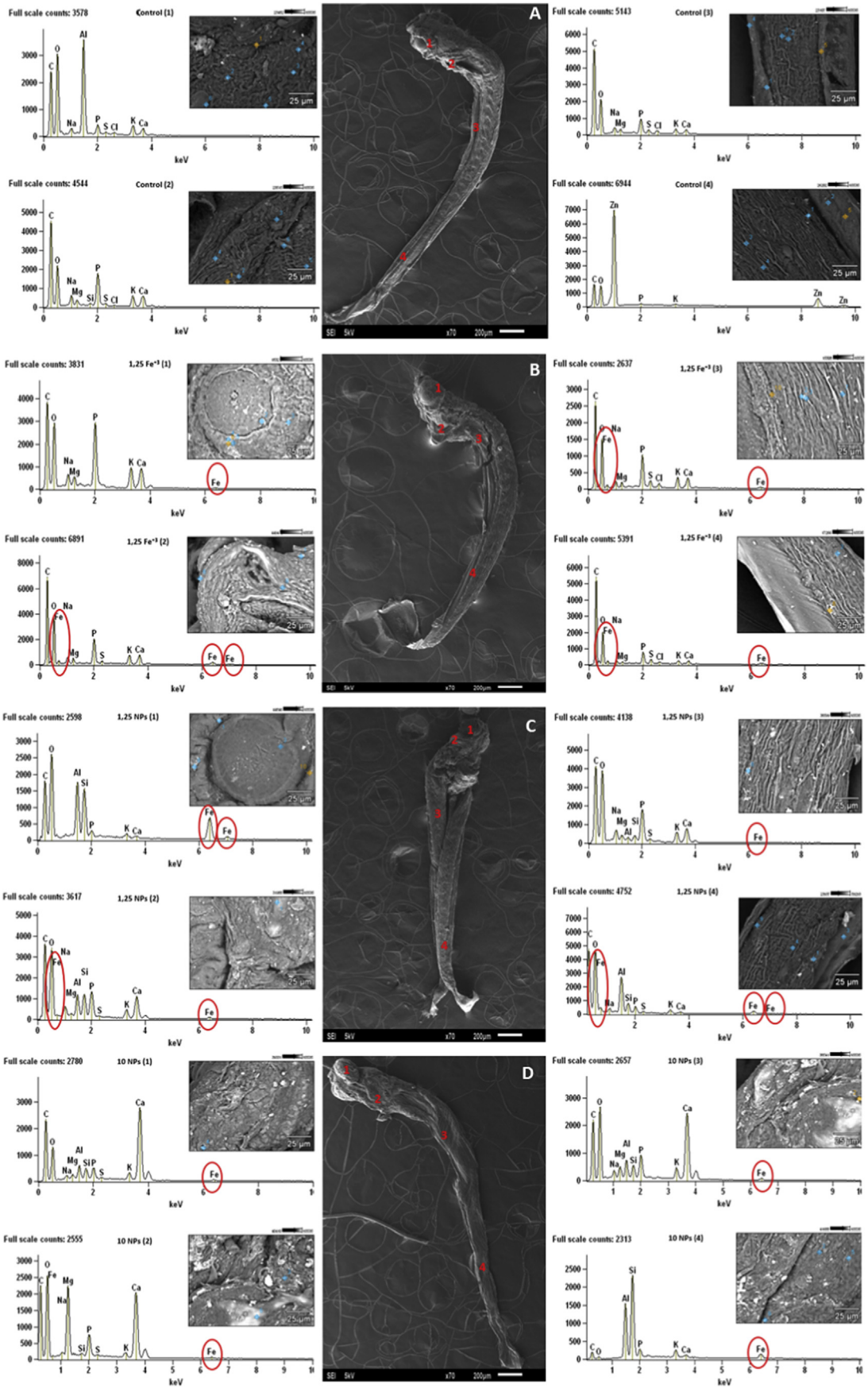

Fig. 4. Scanning Electron Microscopy (SEM) and Energy Dispersive X-Ray Spectroscopy (EDS) of zebrafish larvae from control group and after exposure to γ-Fe_2O_3 nanoparticle (IONPs) and iron ions for 144 h. (A) Control. (B) Iron ions at 1.25 mg L^{-1}. (C) IONP at 1.25 mg L^{-1}. (D) IONP at 10 mg L^{-1}. The numbers indicate the region analyzed in relation to the accumulation. Scale bar = 200 µm.

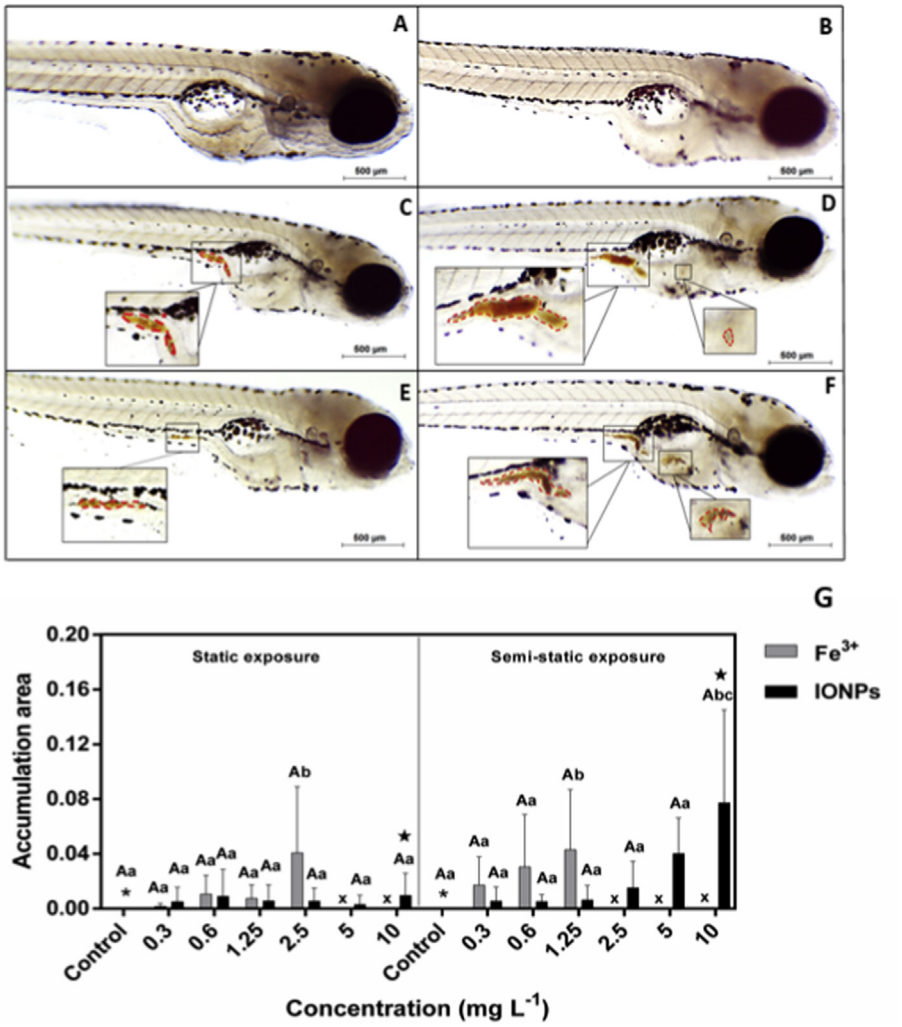

Fig. 5. Photomicrographs of zebrafish larvae after exposure to γ-Fe_2O_3 nanoparticle (IONPs) and iron ions under static and semi-static conditions for 144 h, showing presence of both iron forms in the intestinal tract. (A–B) Control. (C) Iron ion at 1.25 mg L^{-1} under static condition. (D) IONP at 10 mg L^{-1} under static exposure. (E) Iron ions at 1.25 mg L^{-1} under semi-static exposure. (F) IONP at 10 mg L^{-1} under semi-static exposure. Scale bar = 500 μm. (G) Accumulation area in the intestinal tract in zebrafish larvae after 144 h exposure to γ-Fe_2O_3 NPs and iron ions. (*) No accumulation; (star) Difference between static and semi-static exposure. Different capital letters indicate significant differences between IONPs and iron ions at the same concentration. Different lower letters indicate significant differences in the same iron form over concentrations. Results are expressed as mean from 10 larvae.

(Asharani et al., 2008; Powers et al., 2011; Massarsky et al., 2014; Orbea et al., 2017), SiO_2 NPs (Chao et al., 2017) and ZnO NPs (Ong et al., 2013; Chen et al., 2014; Hua et al., 2014; Zhao et al., 2013; Kteeba et al., 2017), confirming that the toxicity of NMs depends on their nano-specific properties (Cheng et al., 2007; Chao et al., 2018; Pereira et al., 2019).

The zebrafish chorion is a barrier that protects the embryo up to 48–72 hpf and has pores with a diameter ranging from 500 to 700 nm, which are important for the oxygen and nutrients transport, and embryo excretion (Rawson et al., 2001). However, pores may facilitate the entry of small NPs (Cheng et al., 2007). When diffused throughout the chorion, these NPs can accumulate and distribute in various embryo organs, causing toxic effects during embryonic development (Chao et al., 2018). The hatching rate in zebrafish involves the expression of specific genes that produce enzymes (i.e. Hgg1 (Cathepsin L, ctslb)) that degrade the chorion facilitating its disruption. NPs can interfere with the expression of the genes responsible for hatching, such as reported for Cu NPs (Zhang et al., 2018), delaying the hatching of embryos (Zhang et al., 2018). Another condition that may interfere with embryo hatching rate is the accumulation of NPs around the chorion that would cause a hypoxic condition and make it difficult to excrete metabolites through the pores, leading to premature hatching of zebrafish embryos (Silva et al., 2018). Neuroactive substances can induce hypoactivity in zebrafish embryos, leading hatching inhibition, such as observed in embryos exposed to Si NPs (62.2 nm; 25–200 μg mL^{-1}, 96 h) (Duan et al., 2013).

3.4.2. Neurotoxicity

After 24 h of exposure, the SCF of embryos exposed to IONPs in static and semi-static conditions was similar to the control group ($p > 0.05$; Fig. 8). However, the semi-static exposure to iron ions at 5.0 mg L^{-1} reduced the SCF when compared to low iron ions concentrations (0.3 and 0.6 mg L^{-1}) and control group ($p < 0.05$; Fig. 8). Changes in spontaneous embryo contraction are indicative of neurotoxicity (Wang et al., 2013; Weichert et al., 2017; Krzykwa et al., 2019) and were associated to alterations in the expression of various genes involved in neural protein synthesis (Fan et al., 2010; Richendrfer and Creton, 2015) or induction of muscle changes (Campos et al., 2015).

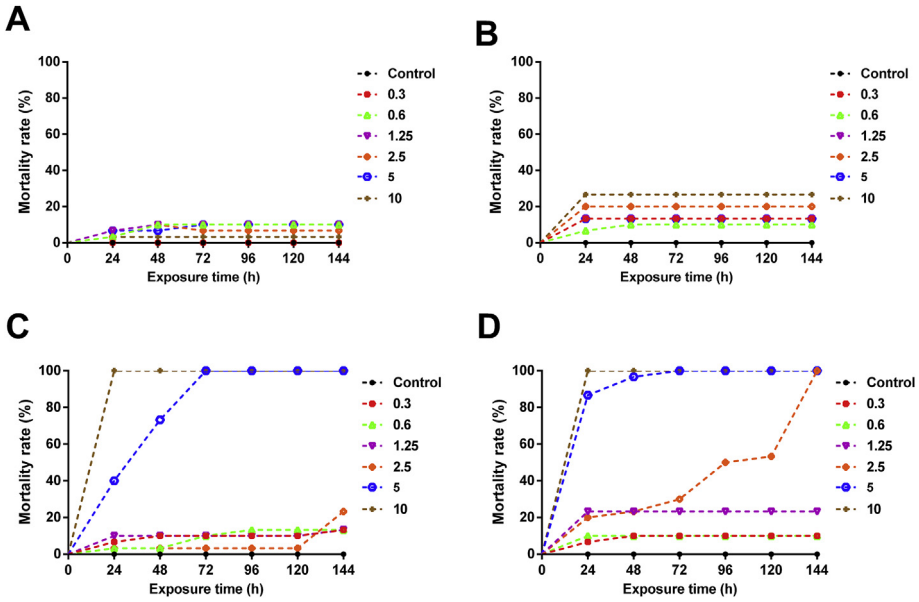

Fig. 6. Mortality rate (%) of zebrafish embryos from control group and after exposure to γ-Fe_2O_3 nanoparticle (IONPs) and iron ions under static (A, C) and semi-static conditions (B, D) for 144 h. (A) Static exposure to IONPs. (B) Semi-static exposure to IONPs. (C) Static exposure to iron ions. (D) Semi-static exposure to iron ions. Results are expressed as mean of triplicates.

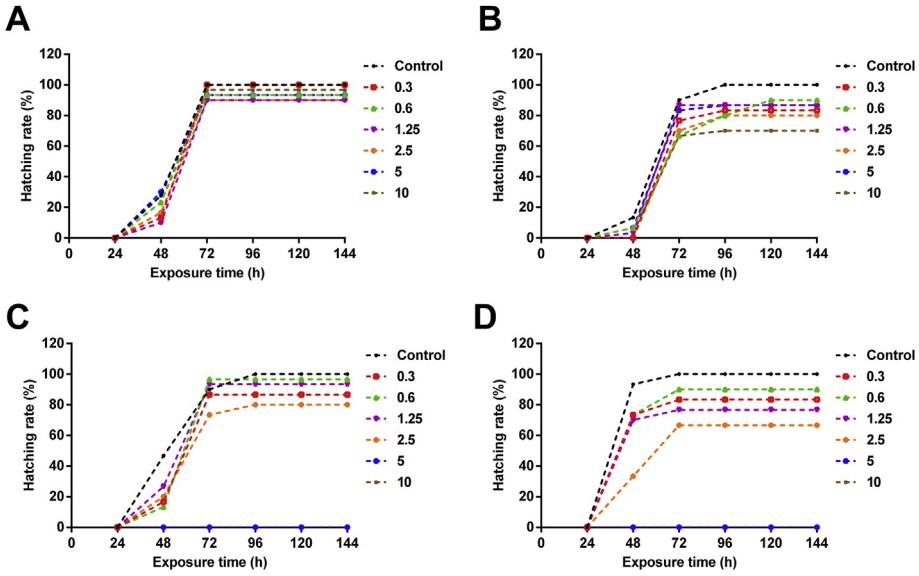

Fig. 7. Hatching rate (%) of zebrafish from control group and after exposure to γ-Fe_2O_3 nanoparticle (IONPs) and iron ions under static (A, C) and semi-static conditions (B, D) for 144 h. (A) Static exposure to IONPs. (B) Semi-static exposure to IONPs. (C) Static exposure to iron ions. (D) Semi-static exposure to iron ions. Results are expressed as mean of triplicates.

Although the neurotoxic effects induced by IONPs in zebrafish has not been described, the ability of amino groups-functionalized γ-Fe_2O_3 NPs (30 nm; 25–200 μg mL^{-1}) to translocate directly from the olfactory nerve to the brain in rats has been reported, reaching the striatum and hippocampus regions, causing neurotoxic effects (Wu et al., 2013). The striatum and hippocampus are important brain structures related to the development of neurodegenerative diseases (Wu et al., 2013). Dopaminergic damage has also been reported in rat brains induced by γ-Fe_2O_3 NPs (10–30 nm; 2.5–40 μg mL^{-1}), revealing a mechanism of neural damage (Imam et al., 2015). In addition, γ-Fe_2O_3 NPs (50 nm; 5 mg kg^{-1} b.w.) exposure induced neurotoxicity and inflammation in rats, causing a decline in the enzymes acetylcholine, esterase, norepinephrine, serotonin, dopamine and antioxidants, increased lipid peroxidation, nitric oxide and p53 tumor suppressor gene, as well as alteration in gene expression of mTFA and PGC-1 α (Yousef et al., 2019a, 2019b).

3.4.3. Cardiotoxicity

Cardiotoxicity was the main toxic effect of both iron forms on the early development of zebrafish (Fig. 9A). After semi-static exposure for 48 h, both iron forms reduced the heart beat rate in zebrafish embryos compared to unexposed ones ($p < 0.05$; Fig. 9A), while no effect was observed after static exposure to γ-Fe_2O_3 NPs

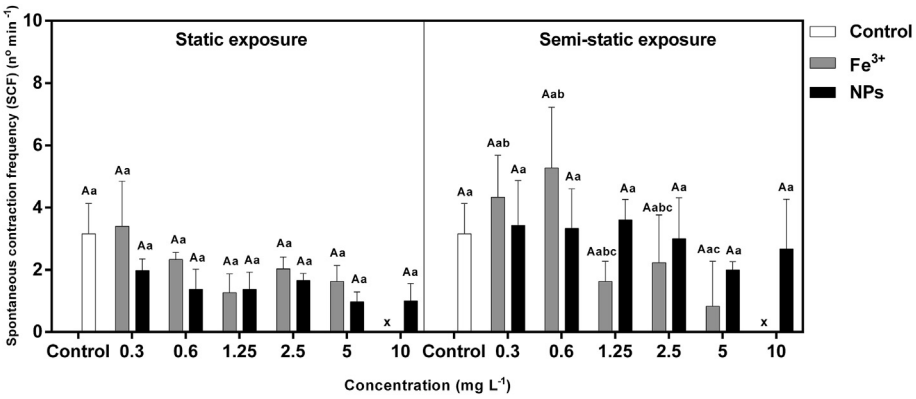

Fig. 8. Spontaneous contraction frequency (SCF) (nº min^{-1}) of zebrafish embryos from control group and after exposure to γ-Fe_2O_3 nanoparticle (IONPs) under static, iron ions under static, IONPs semi-static conditions and iron ions semi-static conditions for 24 h "x" indicated mortality. Different capital letters indicate significant differences between IONPs and iron ions at the same concentration. Different lower letters indicate significant differences in the same iron form over concentrations. Results are expressed as mean and standard deviation of triplicates.

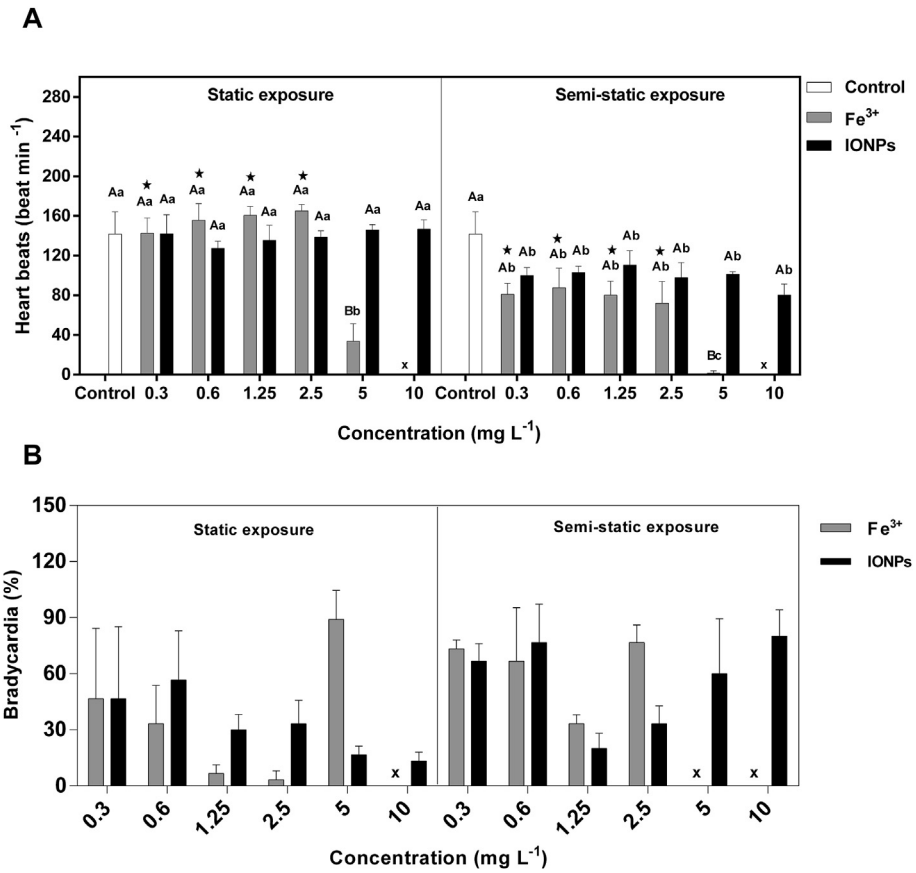

Fig. 9. (A) Heart beat rate (beat min^{-1}) of zebrafish embryos from control group and after exposure to γ-Fe_2O_3 nanoparticle (IONPs) under static, iron ions under static, IONPs semi-static conditions and iron ions semi-static conditions for 48 h "x" indicated mortality. Different capital letters indicate significant differences between IONPs and iron ions at the same concentration. Different lower letters indicate significant differences in the same iron form over concentrations. Star indicates difference between static and semi-static exposure. Results are expressed as mean and standard deviation of triplicates. (B) Frequency (%) of embryos with bradycardia after exposure to static and semi-static exposure to IONPs and iron ions.

($p > 0.05$; Fig. 9A). High frequency of embryos with bradycardia was observed after semi-static exposure to γ-Fe_2O_3 NPs, especially at 0.3 mg L^{-1} (66.6 ± 9.42%), 0.6 mg L^{-1} (76.6 ± 20.54%), 5 mg L^{-1} (60 ± 29.43%) and 10 mg L^{-1} (80 ± 14.14%) at static exposure and at 0.3 mg L^{-1} (46.66 ± 38.58%), 0.6 mg L^{-1} (56.6 ± 26.24%), 1.25 mg L^{-1} (30 ± 8.16%) and 2.5 mg L^{-1} (33.3 ± 12.47%) after static exposure (Fig. 9B). Zebrafish embryos after static exposure to iron ions showed similar heart beat rate to unexposed ones ($p > 0.05$; Fig. 9A). However, significant alterations on heart beat rate were observed after semi-static exposure to iron ions at 0.3 mg L^{-1} ($p = 0.0018$), 0.6 mg L^{-1} ($p = 0.00062$), 1.25 mg L^{-1} ($p = 0.0269$) and 2.5 mg L^{-1} ($p = 0.0038$) (Fig. 9A). The frequency of embryos with bradycardia increased after semi-static exposure to iron ions, mainly at 0.3 mg L^{-1} (73.33 ± 4.71%), 0.6 mg L^{-1} (66.6 ± 28.67%) and

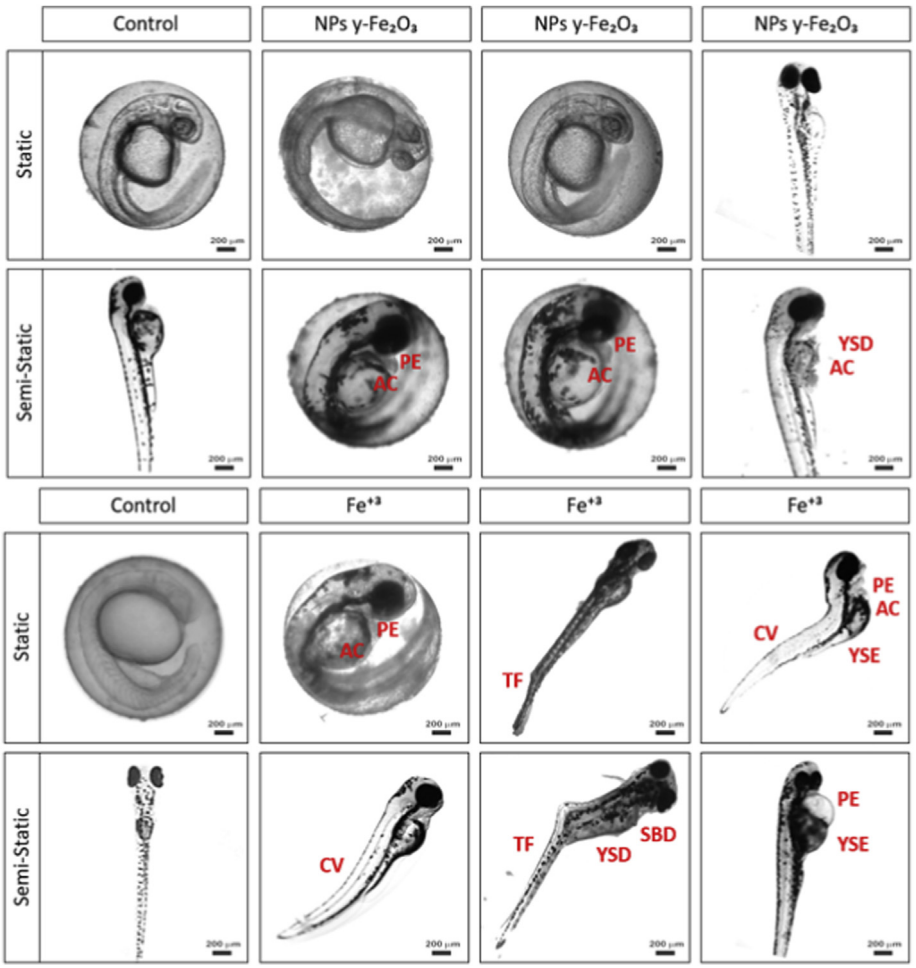

Fig. 10. Photomicrographs of zebrafish embryos and larvae from control group and after exposure to γ-Fe_2O_3 nanoparticle (IONPs) under static (0.3–10 mg L^{-1}), iron ions under static (0.3–2.5 mg L^{-1}), IONPs semi-static conditions (0.3–10 mg L^{-1}) and iron ions semi-static conditions (0.3–1.25 mg L^{-1}) during 144 h. Blood accumulation (AC), pericardial edema (PE), tail flexion (TF) spinal curvature (CV), swim bladder deformity (SBD), yolk sac edema (YSE) and yolk sac deformity (YSD).

2.5 mg L^{-1} (76.66 ± 9.42%) when compared to static exposure to iron ions at 0.3 mg L^{-1} (46.6 ± 37.7%), 0.6 mg L^{-1} (33.3 ± 20.5%) and 2.5 mg L^{-1} (3.3 ± 4.71%) (Fig. 9B), confirming the cardiotoxic effects induced by both iron forms in zebrafish embryos.

Cardiotoxic effects induced by γ-Fe_2O_3 NPs in zebrafish embryos should be related to the release of iron ions, which can induce inflammation, lipid peroxidation (LPO) and oxidative stress, such as observed in BALB/c mice (Bostan et al., 2016). The heart is an organ sensitive to iron accumulation, which induces apoptosis and tissue degeneration, as well reduced heart beat rate (Parkes et al., 1993; Lekawanvijit and Chattipakorn, 2009; Bostan et al., 2016). Dextran, pluronic and polyethylene glycol functionalized IONPs (10–30 nm; 100–500 μg mL^{-1}) accumulation in the heart has been previously reported in BALB/c mice (Feng et al., 2018). Ca^{2+} type L channels provide the main pathway for iron to enter cardiomyocytes, which leads to this iron accumulation (Oudit et al., 2003). The NP accumulation in the heart induced the production of highly toxic hydroxyl radicals through the Fenton-catalysed Haber-Weiss reaction. These free radicals damage the lipid-rich cardiomyocyte cell membrane through LPO, as well as changed Na^+ K^+-ATPase and 5′-nucleotidase. Oxidative stress can also induce cardiomyocyte cell death (Bartfan et al., 1999; Gujja et al., 2010; Kremastinos and Farmakis, 2011; Shen et al., 2015). The oxidative stress in zebrafish embryos also was reported after exposure to Ag NPs (8.39 ± 0.98 nm; 0.03–1.55 μg mL^{-1}) (Massarsky et al., 2013), indicating that the NM-induced cardiotoxicity was mediated by ROS production and oxidative stress.

Similarly, polyacrylic acid-functionalized γ-Fe_2O_3 NPs (6.8 nm) at 10 mg kg^{-1} reduced the heart beat rate in BALB mice after intravenously injection (Iversen et al., 2013). In addition, other metal-based NPs have similar cardiotoxicity mechanisms (Cao et al., 2018). Polyvinyl acetate (PVA)-functionalized Ag NPs (5–35 nm; 10–100 μg mL^{-1}) decreased heart beat rate, pericardial edema and circulatory defects in zebrafish embryos (Asharani et al., 2011), as observed in the present study. Ag NPs also showed direct effects on ion channels, decreasing Na^+ and K^+ transport, reducing the recovery of Na^+ and K^+ channels from cardiomyocytes, causing a decrease in heart beat rate (Lin et al., 2017). Despite the widespread use of zebrafish as an animal model for cardiovascular disease studies (Chico et al., 2008; Houge et al., 2012; Zakaria et al., 2018), the present study is a pioneer in the identification of the IONP-induced cardiotoxicity in zebrafish embryos. Thus, it is emphasized the need for further studies on the effects of γ-Fe_2O_3 NPs on the heart, mainly due to their numerous medical applications.

3.4.4. Morphological alterations and morphometric analysis

Citrate-functionalized γ-Fe_2O_3 NPs induced low frequency of morphological alterations on zebrafish embryo and larvae when compared to iron ions (Fig. 10; see Supplementary Material

Table S1). Furthermore, several morphological alterations were observed in zebrafish embryos exposed to both iron forms in an exposure condition dependent pattern, wherein a larger number of morphological alterations induced by both iron forms was observed after semi-static exposure when compared to static exposure (Fig. 10), confirming the importance of establishing exposure patterns for nanotoxicological tests, such as ZET.

After static exposure, similar frequency of morphological alterations was observed in zebrafish exposed o γ-Fe_2O_3 NPs compared to unexposed ones. However, after semi-static exposure to γ-Fe_2O_3 NPs zebrafish showed pericardial edema, blood accumulation in the heart, spinal curvature, tail deformation, swim bladder deformation and vitelline sac edema (Fig. 10; Table S1). Interestingly, zebrafish embryos exposed to uncoated γ-Fe_2O_3 NPs (30 nm; 0.1–100 mg L^{-1}) under static condition for 168 h showed pericardial edema, tissue ulceration and spinal curvature in zebrafish embryos (Zhu et al., 2012), confirming that unfunctionalized IONPs, even under static conditions, may present higher oxidative dissolution following by ion release, inducing greater embryotoxicity in zebrafish. Similarly, previous studies indicated that the IONP toxicity was associated to NP dissolution and oxidative stress induced by released iron ions (Wang et al., 2013; Patil et al., 2015; Lei et al., 2018). On the other hand, results showed that the iron ions induced several teratogenic effects after both exposure conditions, such as pericardial edema, blood accumulation in the heart, tail deformation, spinal cord curvature, swim bladder deformity, and yolk sac edema, confirming their embryotoxicity after static and semi-static exposure conditions.

Morphometric parameters of zebrafish larvae exposed to both iron forms for 144 h under static and semi-static conditions are shown in the Supplementary Material Table S2. An overview of these results indicates that the IONPs did not change the sensory, muscular structural and skeletal structural parameters after static and semi-static exposures. On the other hand, iron ions changed the physiological parameters after semi-static exposure, such as reduced the swimming bladder area at 1.25 mg L^{-1} ($p = 0.00015$), reduced the area of yolk sac ($p = 0.02659$), change skeletal parameters such as, reduced the head height at 0.3 mg L^{-1} ($p = 0.00548$). Furthermore, the iron ions at 2.5 mg L^{-1} reduced the distance from mouth to anus after static conditions ($p = 0.0365$; Table S2).

Quantitative analysis of morphometric parameters helps to eliminate errors of qualitative analysis, making possible to observe previously subtle morphological change (Hinz et al., 2012). The observed physiological and structural changes in zebrafish larvae after semi-static exposure to iron ions are indicative of somatic and systemic changes. Larva length and natural bladder area are usually the most affected parameters (Teixidó et al., 2018). The development of the swim bladder depends on blood circulation and therefore may have a side effect of changes in vascularization (Yue et al., 2015). Chemicals that affect heart rate, causing bradycardia, usually cause lack of swim bladder inflation (Bittner et al., 2018). As observed in this study, iron ions in semi-static conditions decreased the heart beat rate (Fig. 9A) and induced blood accumulation (Fig. 10), confirming the effect on bladder inflation.

4. Conclusion

The multiple biomarker approach using the ZET, especially the sublethal parameters, allowed the description of the toxicity of iron oxide nanoparticles (IONPs). The hypothesis that the embryotoxicity of citrate-functionalized γ-Fe_2O_3 NPs in zebrafish is dependent on exposure condition was confirmed. In addition, the toxicity of both iron forms (IONPs and iron ions) was concentration and exposure condition dependent, while the γ-Fe_2O_3 NPs showed low embryotoxic effects compared to its dissolved counterpart. However, results indicated sub-lethal effects of citrate-functionalized γ-Fe_2O_3 NPs on zebrafish, specially cardiotoxicity. In summary, under semi-static exposure conditions there was a potentiation of effects induced by citrate functionalized γ-Fe_2O_3 NPs when compared to static exposure. Given the pioneering nature of this study, observed results recommend further research about other types of exposure conditions, such as continuous flow or environmental relevant conditions (i.e., mesocosm or multi-exposure species).

Declaration of competing interest

The authors declare that they have no known competing financial interests or personal relationships that could have appeared to influence the work reported in this paper.

CRediT authorship contribution statement

Aryelle Canedo Pereira: Methodology, Data curation, Writing - review & editing. **Bruno Bastos Gonçalves:** Methodology, Formal analysis. **Rafaella da Silva Brito:** Methodology, Formal analysis. **Lucélia Gonçalves Vieira:** Methodology, Formal analysis. **Emília Celma de Oliveira Lima:** Methodology, Data curation. **Thiago Lopes Rocha:** Conceptualization, Supervision, Data curation, Writing - review & editing.

Acknowledgements

This work was funded by the National Council for Scientific and Technological Development - CNPq (MCTIC/CNPq Nº 28/2018; nº 433553/2018-9) and Coordination of Improvement of Higher Level Personnel – CAPES (nº 88882.386347/2019–01). The authors also acknowledge *Centro Regional para o Desenvolvimento Tecnológico e Inovação* (CRTIUFG), *LaboratórioMultiusuário de Microscopia de Alta Resolução* (LabMic-UFG) and Central analítica IQ-UFG for their collaboration in the characterization of IONPs.

Appendix A. Supplementary data

Supplementary data to this article can be found online at https://doi.org/10.1016/j.chemosphere.2020.126792.

References

Aksakal, F.I., Ciltas, A., 2019. Impact of copper oxide nanoparticles (CuO NPs) exposure on embryo development and expression of genes related to the innate immune system of zebrafish (Danio rerio). Comp. Biochem. Physiol. C 223, 78–87. https://doi.org/10.1016/j.cbpc.2019.05.016.

Asharani, P.V., Serina, N.G.B., Nurmawati, M.H., Wu, Y.L., Gong, Z., Valiyaveettil, S., 2008. Impact of multi-walled carbon nanotubes on aquatic species. J. Nanosci. Nanotechnol. 8, 3603–3609. https://doi.org/10.1166/jnn.2008.432.

Asharani, P.V., Lianwu, Gong, Z., Valiyaveettil, S., 2011. Comparison of the toxicity of silver, gold and platinum nanoparticles in developing zebrafish embryos. Nanotoxicology 5, 43–54. https://doi.org/10.3109/17435390.2010.489207.

Ates, M., Demir, V., Adiguzel, R., Arslan, Z., 2013. Bioaccumulation, subacute toxicity, and tissue distribution of engineered titanium dioxide nanoparticles in goldfish (*Carassius auratus*). J. Nanomater. 460518, 1–7. https://doi.org/10.1155/2013/460518.

Ates, M., Demir, V., Arslan, Z., Kaya, H., Yilmaz, S., Camas, M., 2016. Chronic exposure of Tilapia (*Oreochromis niloticus*) to iron oxide nanoparticles: effects of particle morphology on accumulation, elimination, hematology and immune responses. Aquat. Toxicol. 177, 22–32. https://doi.org/10.1016/j.aquatox.2016.05.005.

Avdesh, A., Chen, M., Martin-Iverson, M.T., Mondal, A., Ong, D., Rainey-Smith, S., Taddei, K., Lardelli, M., Groth, D.M., Verdile, G., Martins, R.N., 2012. Regular care and maintenance of a zebrafish (*Danio rerio*) laboratory: an introduction. J. Vis. Exp. 69, e4169. https://doi.org/10.3791/4196.

Babić, S., Barišić, J., Višić, H., Klobučar, R.S., Popović, N.T., Strunjak-Perović, I., Coz-Klobučar, R., 2017. Embryotoxic and genotoxic effects of sewage effluents in zebrafish embryo using multiple endpoint testing. Water Res. 115, 9–21. https://doi.org/10.1016/j.watres.2017.02.049.

Babić-Stojić, B., Milivojevic, D., Jokanovic, V.R., Pozek, M., 2017. Ultrasmall iron oxide nanoparticles: Magnetic and NMR relaxometric properties. Curr. Appl. Phys. 18, 141–149. https://doi.org/10.1016/j.cap.2017.11.017.

Bartfan, W.J., Dawood, F., Wen, W.H., Lehotay, D.C., Hou, D., Bartfay, E., Luo, X., Backx, P.H., Liu, P.P., 1999. Cardiac function and cytotoxic aldehyde production in a murine model of chronic iron-overload. Cardiovasc. Res. 43, 892–900. https://doi.org/10.1016/s0008-6363(99)00040-1.

Beekhuizen, M., Koning, C., Guillén, M.E.F., Buitenweg, S.V., Kaplon, M.T., Waart, B.V., Emmen, H., 2015. From cutting edge to guideline: a first step in harmonization of the zebrafish embryotoxicity test (ZET) by describing the most optimal test conditions and morphology scoring system. Reprod. Toxicol. 56, 64–76. https://doi.org/10.1016/j.reprotox.2015.06.050.

Bergin, I.L., Witzmann, F.A., 2013. Nanoparticle toxicity by the gastrointestinal route: evidence and knowledge gaps. Int. J. Biomed. Nanosci. Nanotechnol. (IJBNN) 3, 1–2. https://doi.org/10.1504/IJBNN.2013.054515.

Bittner, L., Teixido, E., Seiwert, B., Escher, B.I., Kluver, N., 2018. Influence of pH on the uptake and toxicity of β-blockers in embryos of zebrafish, *Danio rerio*. Aquat. Toxicol. 201, 129–137. https://doi.org/10.1016/j.aquatox.2018.05.020.

Bostan, H.B., Rezaee, R., Valokala, M.G., Tsarouhas, K., Golokhvast, K., Tsatsakis, A.M., Karimi, G., 2016. Cardiotoxicity of nano-particles. Life Sci. 15, 91–99. https://doi.org/10.1016/j.lfs.2016.09.017.

BRASIL, 2011. Resolução CONAMA nº 430, de 13 de maio de 2011. Conselho Nacional do Meio Ambiente: CONAMA, Brasília, DF, maio de.

Brun, N.R., van Hage, P., Hunting, E.R., Haramis, A.P., Vink, S.C., Vijver, M.G., Schaaf, M.J.M., Tudorache, C., 2019. Polystyrene nanoplastics disrupt glucose metabolism and cortisol levels with a possible link to behavioural changes in larval zebrafish. Commun Biol 2, 382. https://doi.org/10.1038/s42003-019-0629-6.

Bugel, S.M., Tanguay, R.L., Planchart, A., 2014. Zebrafish: a marvel of high-throughput biology for 21st century toxicology. Curr. Environ. Health. Rep. 1, 341–352. https://doi.org/10.1007/s40572-014-0029-5.

Cambier, S., Rogeberg, M., Georgantzopoulou, A., Serchi, T., Karlsson, C., Verhaegen, S., Iversen, T.G., Guignard, C., Kruszewski, M., Hoffmann, L., Audinot, J.N., Ropstad, E., Gutleb, A.C., 2018. Fate and effects of silver nanoparticles on early life-stage development of zebrafish (*Danio rerio*) in comparison to silver nitrate. Sci. Total Environ. 610–611, 972–982. https://doi.org/10.1016/j.scitotenv.2017.08.115.

Campos, L.M., Rios, E.A., Midlej, V., Atella, G.C., Houzel-Herculano, S., Benchimol, M., Mermelstein, C., Costa, M.L., 2015. Structural analysis of alterations in zebrafish muscle differentiation induced by simvastatin and their recovery with cholesterol. J. Histochem. Cytochem. 63, 427–437. https://doi.org/10.1369/0022155415580396.

Cao, Y., Gong, Y., Liao, W., Luo, Y., Wu, C., Wang, M., Yang, Q., 2018. A review of cardiovascular toxicity of TiO_2, ZnO and Ag nanoparticles (NPs). Biometals 31, 457–476. https://doi.org/10.1007/s10534-018-0113-7.

Chakraborty, C., Sharma, A.R., Sharma, G., Lee, S.S., 2016. Zebrafish: a complete animal model to enumerate the nanoparticle toxicity. NanoBiotechnology 14–65. https://doi.org/10.1186/s12951-016-0217-6.

Chao, S.J., Huang, C.P., Chen, P.C., Chang, S.H., Huang, C., 2018. Uptake of BDE-209 on zebrafish embryos as affected by SiO_2 nanoparticles. Chemosphere 205, 570–578. https://doi.org/10.1016/j.chemosphere.2018.04.075.

Chao, S.J., Huang, C.P., Chen, P.C., Chihpin, H., 2017. Teratogenic responses of zebrafish embryos to decabromodiphenyl ether (BDE-209) in the presence of nano-SiO2 particles. Chemosphere 178, 449–457. https://doi.org/10.1016/j.chemosphere.2017.03.075.

Chen, L.Q., Ding, C.Z., Ling, J., 2017a. Intensive epidermal adsorption and specific venous deposition of carboxyl quantum dots in zebrafish early-life stages. Chemosphere 184, 44–52. https://doi.org/10.1016/j.chemosphere.2017.05.173.

Chen, T.H., Lin, C.C., Meng, P.J., 2014. Zinc oxide nanoparticles alter hatching and larval locomotor activity in zebrafish (*Danio rerio*). J. Hazard Mater. 277, 134–140. https://doi.org/10.1016/j.jhazmat.2013.12.030.

Chen, G., Vijver, M.G., Xiao, Y., Peijnenburg, W.J.G.M., 2017b. A review of recent advances towards the development of (quantitative) structure-activity relationships for metallic nanomaterials. Materials 10, 1013. https://doi.org/10.3390/ma10091013.

Cheng, J., Flahaut, E., Cheng, S.H., 2007. Effect of carbon nanotubes on development zebrafish (*Danio rerio*) embryos. Environ. Toxicol. Chem. 26, 708–716. https://doi.org/10.1897/06-272R.1.

Cheng, D., Shami, G.J., Morsch, M., Chung, R.S., Braet, F., 2016. Ultrastructural mapping of the zebrafish gastrointestinal system as a basis for experimental drug studies. BioMed Res. Int. 2016, 1–13. https://doi.org/10.1155/2016/8758460.

Chico, T.J., Ingham, P.W., Crossman, D.C., 2008. Modeling cardiovascular disease in the zebrafish. Trends Cardiovasc. Med. 18, 150–155. https://doi.org/10.1016/j.tcm.2008.04.002.

Dammski, A.P., Muller, B.R., Gaya, C., Regonato, D., 2011. Zebrafish: Manual de Criação em Biotério. Universidade Federal do Paraná, Curitiba, pp. 1–107.

Della Torre, C., Maggioni, D., Ghilardi, A., Parolini, M., Santo, N., Landi, C., Madaschi, L., Magni, S., Tasselli, S., Ascagni, M., Bini, L., La Porta, C., Del Giacco, L., Binelli, A., 2018. The interactions of fullerene C_{60} and Benzo(α)pyrene influence their bioavailability and toxicity to zebrafish embryos. Environ. Pollut. 241, 999–1008. https://doi.org/10.1016/j.envpol.2018.06.042.

Duan, J., Yu, Y., Shi, H., Tian, L., Guo, C., Huang, P., Zhou, X., Peng, S., Sun, Z., 2013. Toxic effects of silica nanoparticles on zebrafish embryos and larvae. PloS One 8, 74606. https://doi.org/10.1371/journal.pone.0074606.

Fako, V.E., Furgeson, D.Y., 2009. Zebrafish as a correlative and predictive model for assessing biomaterial nanotoxicity. Adv. Drug Deliv. Rev. 61, 478–486. https://doi.org/10.1016/j.addr.2009.03.008.

Fan, C.Y., Cowden, J., Simmons, S.O., Padilla, S., Ramabhadran, R., 2010. Gene expression. Changes in developing zebrafish as potential markers for rapid developmental neurotoxicity screening. Neurotoxicol. Teratol. 32, 91–98. https://doi.org/10.1016/j.ntt.2009.04.065.

Fatima, H., Kim, K.S., 2018. Iron-based magnetic nanoparticles for magnetic resonance imaging. Adv. Powder Technol. 29, 2678–2685. https://doi.org/10.1016/j.apt.2018.07.017.

Feng, Q., Liu, Y., Huang, J., Chen, K., Huang, J., Xiao, K., 2018. Uptake, distribution, clearance, and toxicity of iron oxide nanoparticles with different sizes and coatings. Sci. Rep. 8, 2082. https://doi.org/10.1038/s41598-018-19628-z.

Fent, K., Weisbrod, C.J., Heller, A.W., Pieles, U., 2010. Assessment of uptake and toxicity of fluorescent silica nanoparticles in zebrafish (*Danio rerio*) early life stages. Aquat. Toxicol. 100, 218–228. https://doi.org/10.1016/j.aquatox.2010.02.019.

Giannaccini, M., Cushieri, A., Dente, L., Raffa, V., 2014. Non-mammalian vertebrate embryos as models in nanomedicine. Nanomedicine 10, 703–719. https://doi.org/10.1016/j.nano.2013.09.010.

Giese, B., Klaessig, F., Park, B., Ralf, K., Steinfeldt, M., Wigger, H., Gleich, A.V., Gottschalk, F., 2018. Risks, release and concentrations of engineered nanomaterial in the environment. Sci. Rep. 8, 1565. https://doi.org/10.1038/s41598-018-19275-4.

Giustini, A.J., Petryk, A.A., Cassim, S.M., Tate, J.A., Baker, I., Hoopes, P.J., 2010. Magnetic naoparticle hyperthermia in cancer treatment. Nano Life 1, 17–32. https://doi.org/10.1142/S1793984410000067.

Gujja, P., Rosing, D.R., Tripodi, D.J., Shizukuda, Y., 2010. Iron overload cardiomyopathy: better understanding of an increasing disorder. J. Am. Coll. Cardiol. 56, 1001–1012. https://doi.org/10.1016/j.jacc.2010.03.083.

Haque, E., Ward, A.C., 2018. Zebrafish as a model to evaluate nanoparticle toxicity. Nanomaterials 8, 561. https://doi.org/10.3390/nano8070561.

Harper, S.L., Carriere, J.L., Miller, J.M., Hutchison, J.E., Maddux, B.L., Tanguay, R.L., 2011. Systematic evaluation of nanomaterial toxicity: utility of standardized materials and rapid assays. ACS Nano 5, 4688–4697. https://doi.org/10.1021/nn200546k.

Hill, A.J., Teraoka, H., Heideman, W., Peterson, R.E., 2005. Zebrafish as a model vertebrate for investigating chemical toxicity. Toxicol. Sci. 86, 6–19. https://doi.org/10.1093/toxsci/kfi110.

Hinz, C., Gebhardt, K., Hartmann, A.K., Sigman, L., Gerlanch, G., 2012. Influence of kinship and MHC class II genotype on visual traits in zebrafish larvae (*Danio rerio*). PloS One 7, 51182. https://doi.org/10.1371/journal.pone.0051182.

Hjorth, R., Coutris, C., Nguyen, H.A., Seycu, A., Urrea, J.A.G., Baun, A., Joner, E.J., 2017. Ecotoxicity testing and environmental risk assessment of iron nanomaterials for sub-surface remediation – recommendations from the FP7 project NanoRem. Chemosphere 182, 525–531. https://doi.org/10.1016/j.chemosphere.2017.05.060.

Houge, T., Ding, Y., Xu, X., 2012. Quantifying cardiac functions in embryonic and adult zebrafish. Methods Mol. Biol. 843, 11–20. https://doi.org/10.1007/978-1-61779-523-7_2.

Howe, K., Clark, M.D., Torroja, C.F., Torrance, J., Berthelot, C., Muffato, M., Collins, J.E., Humphray, S., Mclaren, K., Mathews, L., et al., 2013. The zebrafish reference genome sequence and its relationship to the human genome. Nature 496, 498–503. https://doi.org/10.1038/nature12111.

Hu, J., Wang, D., Wang, J., Wang, J., 2012. Bioaccumulation of Fe2O3(magnetic) nanoparticles in Ceriodaphnia dúbia. Environ. Pollut. 162, 216–222. https://doi.org/10.1016/j.envpol.2011.11.016.

Hua, J., Vijver, M.G., Richardson, M.K., Ahmad, F., Peijnenburg, W.J., 2014. Particle-specific toxic effects of differently shaped zinc oxide nanoparticles to zebrafish embryos (*Danio rerio*). Environ. Toxicol. Chem. 33, 2859–2869. https://doi.org/10.1002/etc.2758.

Imam, S.Z., Lantz-McPeak, S.M., Cuevas, E., Rosas-Hernandez, H., Liachenko, S., Zhang, Y., Sarkar, S., Ramu, J., Robinson, B.L., Jones, Y., Gough, B., Paule, M.G., Ali, S.F., Binienda, Z.K., 2015. Iron oxide nanoparticles induce dopaminergic damage: in vitro pathways and in vivo imaging reveals mechanism of neuronal damage. Mol. Neurobiol. 52, 913–926. https://doi.org/10.1007/s12035-015-9259-2.

ISO 15088, 2007. Water Quality - Determination of the Acute Toxicity of Waste Water to 554 Zebrafish Eggs (*Danio rerio*).

ISO 7346/3, 1996. Water Quality—Determination of the Acute Lethal Toxicity of Substances to a Freshwater Fish [*Brachydanio rerio* Hamilton Buchanan (Teleostei, Cyprinidae)]. Part 3. Flow-Through Method. International Organization for Standardization.

Iversen, N.K., Frische, S., Thomsen, K., Laustsen, C., Pedersen, M., Hansen, P.B., Bie, P., Fresnais, J., Berret, J.F., Baatrup, E., Wang, T., 2013. Superparamagnetic iron oxide polyacrylic acid coated γ-Fe_2O_3 nanoparticles do not affect kidney function but cause acute effect on the cardiovascular function in healthy mice. Toxicol. Appl. Pharmacol. 15, 276–288. https://doi.org/10.1016/j.taap.2012.10.014.

Joo, S.H., Zhao, D., 2017. Environmental dynamics of metal oxide nanoparticles in heterogeneous systems: a review. J. Hazard Mater. 322, 29–47. https://doi.org/10.1016/j.jhazmat.2016.02.068.

Kelkar, D.S., Provost, E., Chaerkady, R., Muthusamy, B., Manda, S.S., Subbannayya, T., et al., 2014. Annotation of the zebrafish genome through an integrated transcriptomic and proteomic analysis. Mol. Cell. Proteomics 13, 3184–3198. https://doi.org/10.1074/mcp.M114.038299.

Kimmel, C.B., Ballard, W.W., Kimmel, S.R., Ullmann, B., Schilling, T.F., 1995. Stages of embryonic development of the zebrafish. Dev. Dynam. 203, 253–310. https://doi.org/10.1002/aja.1002030302.

Kremastinos, D.T., Farmakis, D., 2011. Iron overload cardiomyopathy in clinical practice. Circulation 124, 2253–2263. https://doi.org/10.1161/CIRCULATIONAHA.111.050773.

Krzykwa, J.C., Saeid, A., Jeffries, M.K.S., 2019. Identifying sublethal endpoints for evaluating neurotoxic compounds utilizing the fish embryo toxicity test. Ecotoxicol. Environ. Saf. 170, 521–529. https://doi.org/10.1016/j.ecoenv.2018.11.118.

Kteeba, S.M., El-Adawi, H.I., El-Rayis, O.A., El-Ghobashy, A.E., Shuld, J.L., Svoboda, K.R., Guo, L., 2017. Zinc oxide nanoparticle toxicity in embryonic zebrafish: mitigation with different natural organic matter. Environ. Pollut. 230, 1125–1140. https://doi.org/10.1016/j.envpol.2017.07.042.

Lammer, E., Carr, G.J., Wendler, K., Rawlings, J.M., Belanger, S.E., Braunbeck, T.H., 2009. Is the fish embryo toxicity test (FET) with the zebrafish (*Danio rerio*) a potential alternative for the fish acute toxicity test? Comp. Biochem. Physiol. C Toxicol. Pharmacol. 149, 196–209. https://doi.org/10.1016/j.cbpc.2008.11.006.

Laurent, S., Saei, A.A., Behzadi, S., Panahifar, A., Mahmoudi, M., 2014. Superparamagnetic iron oxide nanoparticles for delivery of therapeutic agents: opportunities and challenges. Expet Opin. Drug Deliv. 11, 1449–1470. https://doi.org/10.1517/17425247.2014.924501.

Lee, W.S., Cho, H.J., Kim, E., Huh, Y.H., Kim, H.J., Kim, B., Kang, T., Lee, J.S., Jeong, J., 2019. Bioaccumulation of polystyrene nanoplastics and their effect on the toxicity of Au ions in zebrafish embryos. Nanoscale 11, 3173–3185. https://doi.org/10.1039/C8NR09321K.

Lei, C., Sun, Y., Tsang, D.C.W., Lin, D., 2018. Environmental transformations and ecological effects of iron-based Nanoparticles. Environ. Pollut. 232, 10–30. https://doi.org/10.1016/j.envpol.2017.09.052.

Lekawanvijit, S., Chattipakorn, N., 2009. Iron overload thalassemic cardiomyopathy: iron status assessment and mechanisms of mechanical and electrical disturbance due to iron toxicity. Can. J. Cardiol. 25, 213–218. https://doi.org/10.1016/s0828-282x(09)70064-9.

Li, H., Zhou, Q., Wu, Y., Fu, J., Wang, T., Jiang, G., 2009. Effects of waterborne nano-iron on medaka (*Oryzias latipes*): antioxidant enzymatic activity, lipid peroxidation and histopathology. Ecotoxicol. Environ. Saf. 72, 634-632. http://dx.10.1016/j.ecoenv.2008.09.027.

Lin, S., Zhao, Y., Nel, A.E., Lin, S., 2013. Zebrafish: an in vivo model for nano EHS studies. Small 9, 1608–1618. https://doi.org/10.1002/smll.201202115.

Lin, C.X., Yang, S.Y., Gu, J.L., Meng, J., Xu, H.Y., Cao, J.M., 2017. The acute toxic effects of silver nanoparticles on myocardial transmembrane potential, I_{Na} and I_{k1} channels and heart rhythm in mice. Nanotoxicology 11, 827–837. https://doi.org/10.1080/17435390.2017.1367047.

Magro, M., Liguoro, M., Franzago, E., Baratella, D., Vianello, F., 2018. The surface reactivity of iron oxide nanoparticles as a potential hazard for aquatic environments: a study on *Daphnia magna* adults and embryos. Sci. Rep. 8, 13017. https://doi.org/10.1038/s41598-018-31483-6.

Malafaia, G., De Souza, A.M., Canedo, P.A., Gonçalves, S., Da Costa Araújo, A.P., Xavier, R.R., Lopes, R.T., 2019. Developmental toxicity in zebrafish exposed to polyethylene microplastics under static and semi-static aquatic systems. Sci. Total Environ. 700, 134867. https://doi.org/10.1016/j.scitotenv.2019.134867.

Malafaia, G., de Souza, A.M., Pereira, A.C., Gonçalves, S., da Costa Araújo, A.P., Ribeiro, R.X., Rocha, T.L., 2020. Developmental toxicity in zebrafish exposed to polyethylene microplastics under static and semi-static aquatic systems. Sci. Total Environ. 700, 134867. https://doi.org/10.1016/j.scitotenv.2019.134867.

Massarsky, A., Dupuis, L., Taylor, J., Eisa-Beygi, S., Strek, L., Trudeau, V.L., Moon, T.W., 2013. Assessment of nanosilver toxicity during zebrafish (*Danio rerio*) development. Chemosphere 92, 59–66. https://doi.org/10.1016/j.chemosphere.2013.02.060.

Massarsky, A., Strek, L., Craig, P.M., Beygi, S.E., Trudeau, V.L., Moon, T.W., 2014. Acute embryonic exposure to nanosilver or silver ion does not disrupt the stress response in zebrafish (*Danio rerio*) larvae and adults. Sci. Total Environ. 478, 133–140. https://doi.org/10.1016/j.scitotenv.2014.01.077.

Moore, M.N., 2006. Do nanoparticles present ecotoxicological risks for the health of the aquatic environment? Environ. Int. 32, 967–976. https://doi.org/10.1016/j.envint.2006.06.014.

OECD, 2013. OECD. OECD Guidelines for the Testing of Chemicals. Section 2: Effects on Biotic Systems Test No. 236: Applicability of the Fish Embryo Acute Toxicity (FET) Test. Organization for Economic Cooperation and Development, Paris, France.

Ong, K.J., Zhao, X., Thistle, M.E., MacCormack, T.J., Clark, R.J., Ma, G., Rubi, Y.M., Simard, B., Loo, J.S.C., Veinot, J.G.C., Goss, G.G., 2013. Mechanistic insights into the effect of nanoparticles on zebrafish hatch. Nanotoxicology 8, 295–304. https://doi.org/10.3109/17435390.2013.778345.

Orbea, A., Soto, N.G., Lacave, J.M., Barrio, I., Cajaraville, M.P., 2017. Developmental and reproductive toxicity of PVP/PEI-coated silver nanoparticles to zebrafish. Comp. Biochem. Physiol. C Toxicol. Pharmacol. 199, 59–68. https://doi.org/10.1016/j.cbpc.2017.03.004.

Oudit, G.Y., Sun, H., Trivieri, M.G., Koch, S.E., Dawood, F., Ackerley, C., Yazdanpanah, M., Wilson, G.J., Schwartz, A., Liu, P.P., Backx, P.H., 2003. L-type Ca2+ channels provide a major pathway for iron entry into cardiomyocytes in iron-overload cardiomyopathy. Nat. Med. 9, 1187–1194. https://doi.org/10.1038/nm920.

Parkes, J.G., Hussain, R.A., Olivieri, N.F., Templeton, D.M., 1993. Effects of iron loading on uptake, speciation, and chelation of iron in cultured myocardial cells. J. Lab. Clin. Med. 122, 36–47.

Patil, U.S., Adireddy, S., Jaiswal, A., Mandava, S., Lee, B.R., Chrisey, D.B., 2015. In vitro/in vivo toxicity evaluation and quantification of iron oxide nanoparticles. Int. J. Mol. Sci. 16, 24417–24450. https://doi.org/10.3390/ijms161024417.

Patil, S.S., Shedbalkar, U.U., Truskewycz, A., Chopade, B.A., Ball, A.S., 2016. Nanoparticles for environmental clean-up: a review of potential risks and emerging solutions. Environ. Technol. Innovat. 5, 10–21. https://doi.org/10.1016/j.eti.2015.11.001.

Pereira, A.C., Gomes, T., Machado, M.R.F., Rocha, T.L., 2019. The zebrafish embryotoxicity test (ZET) for nanotoxicity assessment: from morphological to molecular approach. Environ. Pollut. 252, 1841–1853. https://doi.org/10.1016/j.envpol.2019.06.100.

Pitt, J.A., Kozal, J.S., Javasundara, N., Massarsky, A., Trevisan, G.N., Wiesner, M., Levin, E.D., Giulio, R.T., 2018. Uptake, tissue distribution, and toxicity of polystyrene nanoparticles in developing zebrafish (*Danio rerio*). Aquat. Toxicol. 194, 185–194. https://doi.org/10.1016/j.aquatox.2017.11.017.

Pomeren, M.V., Brun, N.R., Peijnenburg, W.J.G.M., Vijver, M.G., 2017. Exploring uptake and biodistribution of polystyrene (nano)particles in zebrafish embryos at different developmental stages. Aquat. Toxicol. 190, 40–45. https://doi.org/10.1016/j.aquatox.2017.06.017.

Powers, C.M., Slotkin, T.A., Seidler, F.J., Badireddy, A.R., Padilla, S., 2011. Silver nanoparticles alter zebrafish development and larval behavior: distinct roles for particle size, coating and composition. Neurotoxicol. Teratol. 33, 708–714. https://doi.org/10.1016/j.ntt.2011.02.002.

Qualhato, G., Rocha, T.L., Lima, E.C.O., Silva, D.M., Cardoso, J.R., Grisolia, C.K., Sabóia-Morais, S.M.T., 2017. Genotoxic and mutagenic assessment of iron oxide (maghemite-γ-Fe_2O_3) nanoparticle in the guppy *Poecilia reticulata*. Chemosphere 183, 305–314. https://doi.org/10.1016/j.chemosphere.2017.05.061, 2017.

Qualhato, G., Sabóia -Morais, S.M.T., Silva, L.D., Rocha, T.L., 2018. Melanomacrophage response and hepatic histopathologic biomarkers in the guppy *Poecilia reticulata* exposed to iron oxide (maghemite) nanoparticles. Aquat. Toxicol. 198, 63–72. https://doi.org/10.1016/j.aquatox.2018.02.014.

Rawson, D.M., Zhang, T., Kalicharan, D., Jogebloed, W.L., 2001. Field emission scanning electron microscopy and transmission electron microscopy studies of the chorion, plasma membrane and syncytial layers of the gastrula-stage embryo of the zebrafish Brachy *Danio rerio*: a consideration of the structural and functional relationships with respect to cryoprotectant penetration. Aquacult. Res. 31, 325–336. https://doi.org/10.1046/j.1365-2109.2000.00401.x.

Richendrfer, H., Creton, R., 2015. Chlorpyrifos and Malathion have opposite effects on behaviors and brain size that are not correlated to changes in AChE activity. Neurotoxicology 49, 50–58. https://doi.org/10.1016/j.neuro.2015.05.002.

Rubinstein, A.L., 2003. Zebrafish: from disease modeling to drug Discovery. Curr. Opin. Drug Discov. Dev 6, 218–223.

Salieri, B., Turner, D.A., Nowack, B., Hischier, R., 2018. Life cycle assessment of manufactured nanomaterials: where are we? NanoImpact 10, 108–120. https://doi.org/10.1016/j.impact.2017.12.003.

Shen, Y., Huang, Z., Liu, X., Qian, J., Xu, J., Yang, X., Sun, A., Ge, J., 2015. Iron-induced myocardial injury: an alarming side effect of superparamagnetic iron oxide nanoparticles. J. Cell Mol. Med. 19, 2032–2035. https://doi.org/10.1111/jcmm.12582.

Sieber, S., Grossen, P., Bussmann, J., Campbell, F., Kros, A., Witzigmann, D., Huwyler, J., 2019. Zebrafish as a preclinical *in vivo* screening model for nanomedicines. Adv Drug Deliv Ver 151–152, 152–168. https://doi.org/10.1016/j.addr.2019.01.001.

Silva, G.H., Clemente, Z., Khan, L.U., Coa, F., Neto, L.L.R., Carvalho, H.W.P., Castro, V.L., Martinez, D.S.T., Monteiro, R.T.R., 2018. Toxicity assessment of TiO_2-MWCNT nanohybrid material with enhanced photocatalytic activity on *Danio rerio* (Zebrafish) embryos. Ecotoxicol. Environ. Saf. 165, 136–143. https://doi.org/10.1016/j.ecoenv.2018.08.093.

Sobanska, M., Scholz, S., Nyman, A.M., Cesnaitis, R., Alonso, S.G., Ralph, N., Tyle, H., Kenecht, J., Dang, Z., Lundbergh, I., Carlon, C., Coena, W., 2018. Applicability of the fish embryo acute toxicity (FET) test (OECD 236) in the regulatory context of registration, evaluation, authorisation, and restriction of chemicals (REACH). Environ. Toxicol. Chem. 37, 657–670. https://doi.org/10.1002/etc.4055.

Su, C., 2017. Environmental implications and applications of engineered nanoscale magnetite and its hybrid nanocomposites: a review of recent literature. J. Hazard Mater. 322, 48–84. https://doi.org/10.1016/j.jhazmat.2016.06.060.

Suganya, D., Ramakritinan, C.M., Rajan, M.R., 2018. Adverse effects of genotoxicity, bioaccumulation and ionoregulatory modulation of two differently synthesized iron oxide nanoparticles on zebrafish (*Danio rerio*). J. Inorg. Organomet. Polym. Mater. 28, 2603–2611. https://doi.org/10.1007/s10904-018-0935-3.

Teixidó, E., Kiebling, T.R., Krupp, E., Quevedo, C., Muriana, A., Scholz, S., 2018. Automated morphological feature assessment for zebrafish embryo developmental toxicity screens. Toxicol. Sci. 167, 438–449. https://doi.org/10.1093/toxsci/kfy250.

Teja, A.S., Koh, P.Y., 2009. Synthesis, properties, and applications of magnetic iron oxide nanoparticles. Prog. Cryst. Growth Char. 55, 22–45. https://doi.org/10.1016/j.pcrysgrow.2008.08.003.

Truong, L., Happer, S.L., Tanguay, R.L., 2011. Evaluation of embryotoxicity using the zebrafish model. Methods Mol. Biol. 691, 271–279. https://doi.org/10.1007/978-1-60761-849-2_16.

Unal, B., Toprak, M.S., Durmus, Z., Scozeri, H., Baykal, A., 2010. Synthesis, structural and conductivity characterization of alginic acid-Fe_3O_4 nanocomposite. J. Nanoparticle Res. 12, 3039–3048. https://doi.org/10.1007/s11051-010-9898-1.

Underwood, A.J., 1997. Experiments in Ecology: Their Logical Design and Interpretation Using Analysis of Variance. Cambridge University Press, Cambridge.

Vikram, S., Vasanthakumari, R., Tsuzukib, T., Rangarajanc, M., 2017. Hydrodynamics of superparamagnetic iron oxide nanoparticles. Mater Today Proc 4, 10524–10528. https://doi.org/10.3390/ma12111793.

Voinov, M.A., Pagán, J.O.S., Morrison, E., Smirnova, T.I., Smirnov, A.I., 2011. Surface-mediated production of hydroxyl radicals as a mechanism of iron oxide nanoparticle biotoxicity. J. Am. Chem. Soc. 133, 35–41. https://doi.org/10.1021/ja104683w.

Wang, X., Dong, Q., Chen, Y., Jiang, H., Xiao, Q., Wang, Y., Li, W., Bai, C., Huang, C., Yang, D., 2013. Bisphenol A affects axonal growth, musculature and motor behavior in developing zebrafish. Aquat. Toxicol. 15, 104–113. https://doi.org/10.1016/j.aquatox.2013.07.011.

Wehmas, L.C., Anders, C., Chess, J., Punnoose, A., Pereira, C.B., Greenwood, J.A., Tanguay, R.L., 2015. Comparative metal oxide nanoparticle toxicity using embryonic zebrafish. Toxicol. Report. 2, 702–715. https://doi.org/10.1016/j.toxrep.2015.03.015.

Weichert, F.G., Floeter, C., Artmann, A.S., Kammann, U., 2017. Assessing the ecotoxicity of potentially neurotoxic substances e Evaluation of a behavioural parameter in the embryogenesis of Danio rerio. Chemosphere 186, 43–50. https://10.1016/j.chemosphere.2017.07.136.

Wu, J.Q., McCormick, C.D., Pollard, T.D., 2008. Counting proteins in living cells by quantitative fluorescence microscopy with internal standards. Chapter 9. Methods Cell Biol. 89, 253–273.

Wu, J., Ding, T., Sun, J., 2013. Neurotoxic potential of iron oxide nanoparticles in the rat brain striatum and hippocampus. Neurotoxicology 34, 243–253. https://doi.org/10.1016/j.neuro.2012.09.006.

Wu, W., Wu, Z., Yu, T., Jiang, C., Kim, W., 2015. Recent progress on magnetic iron oxide nanoparticles: synthesis, surface functional strategies and biomedical applications. Sci. Technol. Adv. Mater. 16, 023501 https://doi.org/10.1088/1468-6996/16/2/023501.

Xu, P., Zeng, G.M., Huang, D.L., Feng, C.L., Hu, S., Zhao, M.H., Lai, C., Wei, Z., Huang, C., Xie, G.X., Liu, Z.F., 2012. Use of iron oxide nanomaterials in wastewater treatment: a review. Sci. Total Environ. 424, 1–10. https://doi.org/10.1016/j.scitotenv.2012.02.023.

Yang, L., Kuang, H., Zhang, W., Aguilar, Z.P., Xiong, Y., Lai, W., Xu, H., Wei, H., 2015. Size dependent biodistribution and toxicokinetics of iron oxide magnetic nanoparticles in mice. Nanoscale 7, 625–636. https://doi.org/10.1039/c4nr05061d.

Yang, Y., Qin, Z., Zeng, W., Yang, T., Cao, Y., Mei, C., Kuang, Y., 2017. Toxicity assessment of nanoparticles in various systems and organs. Nanotechnol. Rev. 6, 279–289. https://doi.org/10.1515/ntrev-2016-0047.

Yousef, M.L., Abuzr eda, A.A., Kamel, M.A.E.N., 2019b. Cardiotoxicity and lung toxicity in male rats induced by long-term exposure to iron oxide and silver nanoparticles. Exp Ther Med 18, 4329–4339. https://doi.org/10.3892/etm.2019.8108.

Yousef, M.I., Abuzreda, A.A., Kamel, M.A.E.N., 2019a. Neurotoxicity and inflammation induced by individual and combined exposure to iron oxide nanoparticles and silver nanoparticles. J. Taibah Univ. Sci. 13, 570–578. https://doi.org/10.1080/16583655.2019.1602351.

Yue, M.S., Peterson, R.E., Heideman, W., 2015. Dioxin inhibition of swim bladder development in zebrafish: is it secondary to heart failure? Aquat. Toxicol. 162, 10–17. https://doi.org/10.1016/j.aquatox.2015.02.016.

Zakaria, Z.Z., Benslimane, F.M., Nasrallah, G.K., Shurbaji, S., Younes, N.N., Mraiche, F., Da'as, S.I., Yalcin, H.C., 2018. Using zebrafish for investigating the molecular mechanisms of drug-induced cardiotoxicity. BioMed Res. Int. 1642684, 1–10. https://doi.org/10.1155/2018/1642684.

Zhang, Y.J., Zhang, R.T., Sun, H.J., Chen, Q., Yun, X., Zhang, T., Yi, M., Liu, J.X., 2018. Copper inhibits hatching of fish embryos via inducing reactive oxygen species and down-regulating Wnt signaling. Aquat. Toxicol. 205, 156–164. https://doi.org/10.1016/j.aquatox.2018.10.015.

Zhao, X., Wang, S., Wu, Y., You, H., Lv, L., 2013. Acute ZnO nanoparticles exposure induces developmental toxicity, oxidative stress and DNA damage in embryo-larval zebrafish. Aquat. Toxicol. 136–137, 49–59. https://doi.org/10.1016/j.aquatox.2013.03.019.

Zhu, X., Tian, S., Cai, Z., 2012. Toxicity assessment of iron oxide nanoparticles in zebrafish (*Danio rerio*) early life stages. PloS One 7, 46286. https://doi.org/10.1371/journal.pone.0046286.

Zia, M., Phull, A.R., Ali, J.S., 2016. Challenges of iron oxide nanoparticles. Nanotechnol. Sci. Appl. 19, 49–67. https://doi.org/10.2147/NSA.S99986.